CHAPTER 1

INTRODUCTION

1.1 Introduction

Due to the rapid development of modern technology, recent electronics devices generate an enormous amount of heat, which disturbs the normal performance of the devices and reduces their reliability. When a machine operates continuously at any given load, a steady-state temperature distribution is established in the machine such that the heat generated within the machine is equal to the heat transferred from the machine to the surrounding medium. The temperature rise has to be limited for two reasons: mechanical stress and the deterioration of the insulating materials. In electrical motors, the generated heat is varied and it is depend to the size and the work load of the specific motors. Example, the motors which used in industries are specifically made for heavy duties and the heat generation of these motors is very high and it could damage the internal parts and cause the efficiencies to drop. Heat generation is also caused the life span of the motors to decrease and its cause a new replacement which normally cost high.

Therefore, an efficient cooling system is one of the most important problems in designing an electrical motor. There have been numerous attempts to remove high heat flux effectively including natural convection, forced convection, through ventilation, water jackets, submersible, wet rotor and wet stator, spray cooling, radiation and conduction. Due to its simple application, air cooling has been the most widely used cooling technique for electrical motors. Air cooling is usually used with fin-array heat sinks which extend the heat dissipating surface area. The heat generated from the surface is carried out by the air flows by naturally or by forced air convection.

But air cooling has certain limitations where the heat transfer coefficient and heat capacity of air is much lower than the liquid forced convection. Liquid such as water has high heat transfer coefficient than the air and it can dissipate more heats than which done by the air. To improve the heat transfer rate, the water or the other liquids such as ethylene glycol were dispersed and suspended with nanoparticles. This new class of heat transfer fluids is called nanofluids where the high thermal conductivity solid particles were mixed into the heat transfer liquids. According to the effective medium theory for calculation of the mixture thermal conductivity, the thermal conductivity of the solid particle laden fluid is expected to be higher than the pure liquid (Chopkar *et al.,* 2006). Early studies were performed with millimeter sized particles and showed some increase in thermal conductivity. However, the application was hampered by the some problems, such as abrasion, channel clogging due to poor mixing, and severe pressure drops. Due to higher heat transfer rates, nanofluids have attracted much attention from researchers as a new generation of heat transfer fluid for various applications such as automotives, manufacturing and electronics.

1.2 Background of Problem

Currently electrical motors have promised efficiency from 50% to 100% but practically it can be found within the range of 75% to 95%. From the electric motors efficiency equation;

$$\text{efficiency}, \eta = \frac{\text{P out}}{\text{P input}} = \frac{\text{P mechanical}}{\text{P electrical}} \quad (1.1)$$

Where, efficiency is determined by the mechanical power over electrical power (source). But in real cases, few percentages of the input power (electrical power) were released to surrounding as heat energy and it caused drop in output power (mechanical power). To increase the mechanical power and reduce the heat to surrounding, a better cooling system is needed.

The cooling systems which using fins and micro channels are already reached to its limit (Kurkani, *et al.*,2008) and enlarging the heat transfer rate by increasing the area also seemed unsuitable due to it will increase the size of the system (Keblinski et al.,2005). The only option seems to be good is liquid cooling system and the heat transfer rate is depend to the liquid's heat transfer coefficient; *k* where high *k* will caused high thermal conductivity. The current heat transfer fluids such as water and ethylene glycol have low thermal conductivities and as a result there is a demand for new and innovative heat transfer fluid which is able to improve the heat transfer rate in electric motors cooling system.

Nanofluids seemed to have potential of replacing conventional coolant in electric motors cooling system. There have been considerable reports which have shown that nanofluids can enhance convective heat transfer coefficients. 15-40% of heat transfer enhancement can be achieved by using various type of nanofluids (Yu *et*

al.,2007). By improving the heat transfer rate, the size and weight of a electric motors can be reduced where previously bigger sized motors where used to transfer high mechanical power due to high in heat losses. More mechanical power would be generated when the heat losses become minimum and it is directly improve in energy saving. A better thermal management for the electric motors is essential for improving the motors life span by controls the mechanical stress and the deterioration of the insulating materials.

Therefore, this study attempts to find out the heat transfer characteristic of nanofluids as coolant fluid. Thermal performance of nanofluids compared to the conventional coolants and the effects of volume fraction of the nanoparticles to the thermal performances.

1.3 Statement of the Problem

This study is aimed to find out the answers for the following questions;

(a) Is the nanofluids is better alternative way of cooling for electric motors.

(b) What would be the thermal performances of electric motors when using ethylene glycol based aluminum oxide (Al_2O_3) nanofluid as the coolant compared to the ethylene glycol base fluid coolant in electric motors?

(c) Influences on heat transfer rates when using Ethylene glycol based aluminum oxide nanofluids as a coolant.

1.4 Objective of Study

The objectives of the study are as follow:

(a) To determine potential benefits can be achieved when using ethylene glycol based aluminum oxide (Al_2O_3) nanofluids for the cooling in electric motors.

(b) To compare heat transfer performances using ethylene glycol based aluminum oxide nanofluid with conventional coolants such as ethylene glycol.

1.5 Importance of the Study

As stated earlier, the traditional approach of increasing the cooling rate by using geometry modification and improvement are already reached to its limits. The emerging of nanofluids as coolant fluid with higher thermal conductivity is seem suitable to replace water or conventional coolants in automotives, electronics and manufacturing applications. In-depth studies and experiments need to be done before it can fully implemented in industries. However, high cost of nanofluids production may hinder this effort. Analytical analysis can be considered as initial study to determine the performance of nanofluids in any applications including for electric motors cooling. The data from the analytical study can be used to justify the suitability of nanofluids as coolant fluid. If the data shows substantial improvement, experiment can be done to validate the analytical result. In this study, it focuses on the analytical study of thermal performance of electric motors using nanofluids.

1.6 Scope of the Study

Below are the included scopes

(a) Coolants that focused in this study are nanofluids.

(b) Application of nanofluids in electrical devices such as electric motors is emphasized in this study.

(c) Only analytical studies are done to investigate the thermal performances when using nanofluids.

(d) Relevant input data such as thermal performance formulas, properties of nanofluids and etcs required for the calculations are obtained from literatures and calculated from empirical correlations.

(e) The calculations assume that other factors such as thermophysical properties of nanofluids remain constant.

CHAPTER 2

Literature Review

This chapter reviews relevant literatures on electric motors which can be seen commonly in industries and nanofluids. Section 2.1 reviews how the electric motors works and generate heats. It covers thermal characteristics of the motors and heat sources in electric motors. Some of the current cooling methods of electric motors also were discussed. In section 2.2 the fundamental of nanofluids were discussed. It covers the preparation of nanofluids, convection and viscosity of nanofluids and heat transfer variables of nanofluids.

2.1 Electric motors and the cooling methods

2.1.1 How does an electric motor works and generates heat

From the handbook of electric motors it is stated that, the simple magnetic fields push against one another and turn the motor shaft. To create the opposing magnetic fields a current is passed through a wire. This generates a magnetic field around the

wire. By bundling the wire around steel laminations the field strength increases. By arranging the bundles adjacent to magnets, the field generated by the coils interacts with that of the magnets. If the poles of the two fields are the same they will repel each other and tend to move apart. By holding either the magnet or coil still and mounting the other on a shaft which can rotate the magnetic repulsion is captured as rotation.

The force with which it turns is called torque. The amount of torque is always proportional to the current or amps run through the wiring. That means in a given motor 1 amp of current always generates X units of torque and 50 amps always generate $50X$ units of torque. This characteristic is constant for a motor regardless of the voltage level and is known as the torque constant or K_t and expressed as in/oz/amp or mm/N/amp.

The speed at which the motor rotates is related to the voltage used. However voltage is only potential energy and the actual rpm a voltage will create is determined by how many turns of wire there are in each coil and magnet strength. More turns and stronger magnets mean fewer rpm's per volt. Weaker fields mean more rpm's per volt. This characteristic is the voltage constant or K_v. It is expressed as the rpm/V of the motor.

As the parts of the motor which determine the torque, the windings and magnets also affect how fast the motor turns. In a perfect motor they would have no affect and 100% of the energy put in would be put out at the shaft. However losses due to electrical resistance in the wire, the steel in the motor reacting against changes in magnetic fields and parasitic drag in the moving parts mean a motor is less than 100% efficient.

The efficiency of a motor is known at 'eta' and is expressed as a percentage e.g. 90% when 90% of the input is converted to power. Together the inputs: voltage and

current, and the efficiency, determine the power output of a motor which is expressed as Watts. Power is calculated by the formula Volts x Amps x motor efficiency, for an example, Power = 12V x 10A x 0.90 = 108 Watts output (losses = 12W)

The energy which isn't converted into motion becomes heat. This heat, or rather the amount of heat relative to the motors ability to cool itself (surface area and mass), determines how much power the motor can be made without causing damage. This is because if the motor becomes too hot, the electrical resistance increases, heating increases further and magnets lose their strength and motor wires melt. Also a motor remaining at high temps may fail because the modern adhesives use to construct it suffer heat induced fatigue and the magnets separate from the casing or shaft. At high speed the collision of magnets and coils short the wiring leading to a catastrophic failure of the speed controller and battery.

To overcome the heating problems, an effective cooling method is needed where the cooling method not only is considered by the heat level but also the other operating conditions are involved. Cooling system of electric machines is inevitably related to the type of enclosure used in electric machines. Conventionally it is classified by direct and indirect cooling systems. In the former the ambient air is in direct contact with the main heat sources, which are winding and core, while in the latter the main heat sources are completely surrounded by enclosure.

In direct cooling systems, the heat is dissipated by direct convection from the surface of winding and core while in indirect cooling systems the heat is conducted through the enclosed frame and dissipated at the outer surface of the enclosure. This classification of direct and indirect cooling corresponds to two different types of enclosure: the open and the closed, respectively but open enclosure types not widely used because they provide less or no protection to the active parts of the machines.

In closed types enclosure, all the heat only can be dissipated by convection at the outer surface of the enclosure. Sometimes an internal fan is installed to increase the rate of heat flow from the inner parts to the outer surface of the machine. Similarly an external fan is installed to increase the amount of heat through convection at the outer surface, which is termed as forced external cooling. For the most severe thermal conditions, incompressible fluids such as oils or high heat conducting fluid such as nanofluids may be adopted instead of air where several studies and researches were confirmed that nanofluids are most effective fluids to conducting heat.

2.1.2 Heat sources in motors.

There are two main heat sources in electric motors. The first one is, which is most important one is called copper loss, which is the heat generated at coils. The other kind of heat source is usually called a iron loss, which is the sum of the heat dissipated at the motor core made of steel, thus sometime called a core loss. Certainly there are other sources of heat generation such as mechanical friction in bearings but these will be ignored since their contribution to the heat generation are too small compared to the main two.

2.1.2.1 The total copper losses, Q_c

The total copper losses, Q_c of a motor can be calculated by multiplying the number of phase N, by the copper loss in each phase of coil:

$$Q_c = N \times I^2 R = N I^2 \rho \frac{L}{A} \quad (2.1)$$

Where I is the phase current, R is the phase resistance, ρ is the resistivity, A is the cross sectional area of wire and L is the length of the phase. Its shows that, the total copper losses are proportional to the volume of the coils and the current, I is time-averaged. So if a phase current is periodic with the period T, then,

$$Q_c = \frac{N}{T} \int_0^T I^2(t) R \, dt \quad (2.2)$$

And when the current is sinusoidal with the amplitude, I_0 the I is equal to $\frac{I_0}{\sqrt{2}}$.

When the current flows in coils, it will generate heat and increase the coils temperature which is in turn rise the resistance of the coils. It is known that the resistance of the coils increases with temperature, T in ℃ by:

$$R(t) = R_{20} \, [1 + \alpha(T - 20)] \quad (2.3)$$

Where α is the thermal coefficient of resistivity and R_{20} is the resistance at 20℃ (Chai *et al.*, 1998).

The thermal coefficients are:

$\alpha = 0.0039/℃$, for copper wire (99.5% pure)

$\alpha = 0.0041/℃$, for aluminum wire (99.5% pure)

Thus, if the temperature rise at coils is 100℃, then the phase resistance which is linearly proportional to the copper losses Q_c is increased by about 40%. This is cannot be negligible when a harsh load condition is imposed.

2.1.2.2 The iron losses, Q_i

Iron losses are the heats dissipated at the stator and rotor of an electric motor. It is composed by three different components which are: hysteresis loss, eddy current loss and residual loss.

The hysteresis loss occurs in magnetic steel where it changes the magnetic states of the electric motor, while the flux density, B varies. This loss is proportional to the area encircled by the upper and the lower traces of the hysteresis loop. The area can be obtained by an integration and is proportional to B^2. Furthermore, if the shape of the loop remains the same for each cycle, the loss power is simply the product of the area and frequency. Therefore, the hysteresis loss is directly proportional to frequency f and the square of peak flux density B^2 (Tan *et al.*, 1995). Figure 2.1 shows an example of hysteresis loops of a magnetic steel.

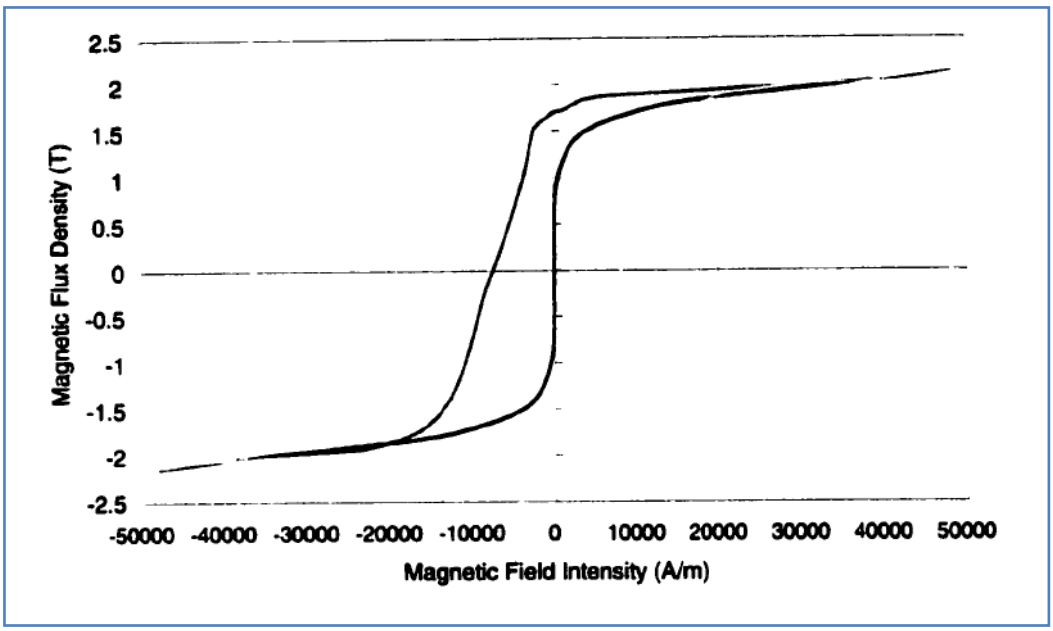

Figure 2.1: Hysteresis loops of the magnetic steel (Tan *et al.*, 1995)

The eddy current loss is also caused by variation in flux densities where it induces currents in materials with finite conductivity at the same frequency as the variation in the magnetic field (Deng *et al.*, 1999).

This loss is some sort of ohmic loss. To reduce eddy current, materials with low resistivity are preferred such as ferrite. Since the mechanism for eddy current loss is the same as that in a conductor, the eddy current loss is proportional to the square of frequency and the square of peak flux density.

The residual loss or anomalous loss is simply taken from experiences that it is proportional to frequency and peak flux density.

Since all the three losses are related to frequency, f and peak flux density, B, the following empirical formula is used to model the iron losses,

$$Q_i = k_h f B^2 + k_e f^2 B^2 + k_r f B \qquad (2.4)$$

Where, $k_{h,} k_e$ and k_r are coefficients of hysteresis, eddy current and residual losses respectively.

2.2 Compact Heat Exchanger for Motor Cooling

Compact heat exchanger is taken into this study to dissipate the heat generations. It is a unique and special class of heat exchanger which used to achieve large heat transfer area per unit volume. Typical surface area to volume ratio for compact heat exchanger is $\geq 400 m^2/m^3$ for liquids and $\geq 700 m^2/m^3$ for gases (Incopera *et al.*, 2007). Several considerations must take into account when designing compact heat exchanger. There are heat transfer surface area, heat transfer rate between the fluids, mechanical

pumping power, friction, pressure drop and velocities of the fluids and etc. These lead to development of several compact heat transfer surfaces as shown in Figure 2.2

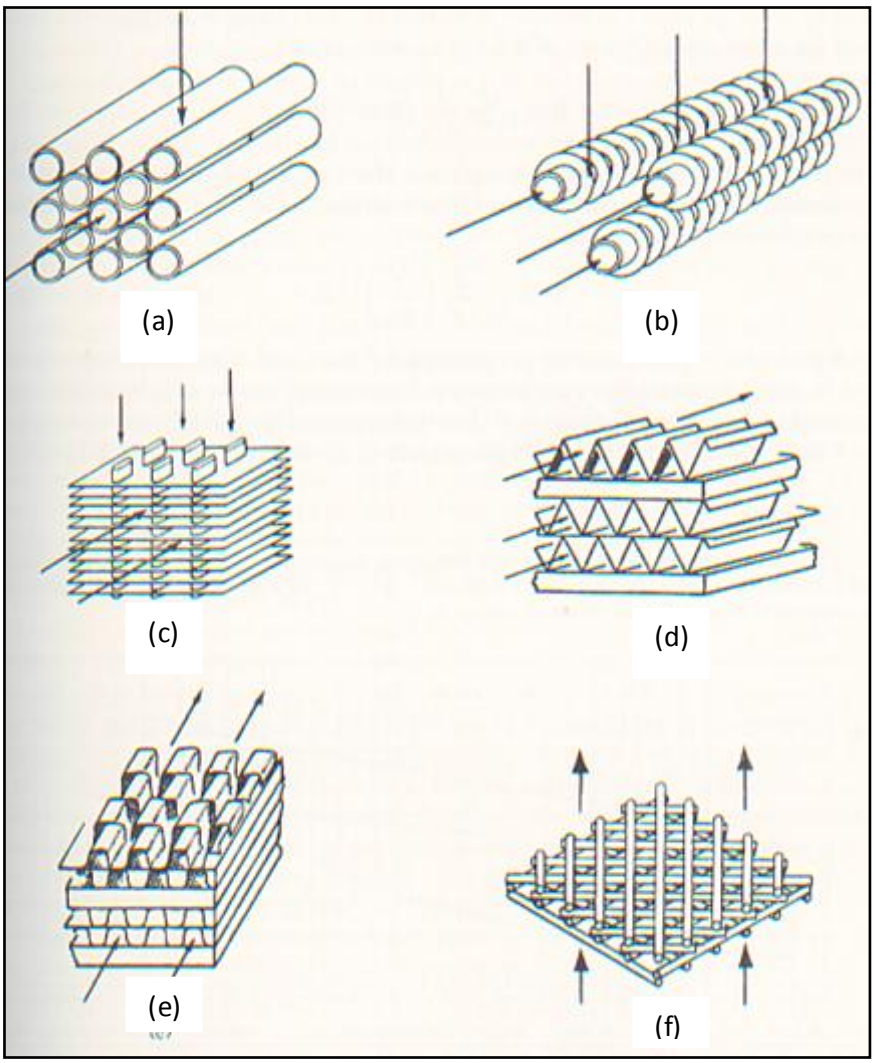

Figure 2.2 Examples of Compact Heat Exchanger Surfaces (Kays & London, 1984)

Each of the surfaces has their advantages and disadvantages. Flat tube as shown in Figure 2.2(c) is more popular for heat transfer applications due to its lower profile drag compared with round tube (Vasu *et al.*,2008). In this compact heat exchanger, both coolant and air flow are unmixed where they flow cross each other.

In the next sections, the fundamental of nanofluids, its properties, experimental and theoretical researches are discussed

2.3 Introduction to Nanofluids

There have been numerous efforts seeking innovative heat transfer liquids as well as improvements in the cooling system to handle continual increases in the heat dissipation in electronic devices such as electric motors. One proposed method is to include high thermal conductivity solid particles into the heat transfer liquids. According to the effective medium theory for calculation of the mixture thermal conductivity, the thermal conductivity of the solid particle laden fluid is expected to be higher than the pure liquid. Early studies were performed with millimeter sized particles and showed some increase in thermal conductivity. However, the application was hampered by the some problems, such as abrasion, channel clogging due to poor mixing, and severe pressure drops. A recent development in modern nanotechnology has enabled researchers to manufacture nanoscale metallic or nonmetallic particles. Nanofluids were invented by incorporating these nanoscale solid particles into ordinary liquids. The term 'Nanofluids' was first introduced by Choi and coworkers at Argonne National Laboratory (Eastman et al., 1996). Nanofluids consist of small fractions of nanoscale solid particles (dp <100nm) or nanotubes in base fluids such as water or oil. Some examples of nanofluids are aluminum oxide particles in deionized water, copper oxide particles in ethylene glycol and carbon nanotubes in oil. Nanofluids have the potential to offer higher thermal conductivity compared to the base fluids themselves. A number of thermal conductivity measurements on stationary nanofluids have been performed since 1995; thermal conductivity increases of up to 60% have been reported

with 5 volume % CuO nanoparticles (Eastman et al., 1996). Many of the measured thermal conductivity values are much greater than predicted by effective medium models.

Other advantages of nanofluids as heat transfer fluid are the fact that nanofluids are not expected to cause clogging or abrasion problems in flow channels, and excellent stability is expected due to the small particle size. Therefore, the use of nanofluids to replace traditional heat transfer fluids, such as water, oil and ethylene glycol, may offer the potential to increase the performance of liquid cooling systems without increasing the complexity.

There are a number of problems in the application of nanofluids at the moment. Previous measurements of the thermal conductivity of stationary nanofluids are very widely scattered, despite the fact that the same particle materials and same measurements techniques are used. These inconsistencies are discussed extensively in the review paper by Kabelac & Kuhnke (2006). Inconsistencies are also found in the relatively few experiments on nanofluid convective heat transfer and viscosity. Convective heat transfer rates and viscosity of nanofluids are very critical because they determine the capability of nanofluids as heat transfer liquids in heat exchangers. Nevertheless, there has been little research on these, so further study is required to completely understand the nanofluid behavior.

Numerous efforts have been devoted to the theoretical study to explain the anomalous increase in nanofluid thermal conductivity. The proposed reasons are Brownian motion of the particles, molecular level layering of the liquid at the liquid/solid interface, and the effects of nanoparticle clustering. Based on the past studies, nanofluid performance is a function of various parameters, such as particle material, particle diameter, particle aggregation, pH of the suspension, temperature of

the suspension and so on. This complexity makes it difficult to predict nanofluid behavior. Moreover, there is so much variability among different experiments that the theorist does not have a reliable basis for testing models.

2.2.1 Preparation of nanofluids

Nanoparticles which are used in nanofluids can be classified by the materials. The most frequently used materials are oxide nanoparticles, such as aluminum oxide (Al203) and copper oxide (CuO). The second kind materials are metallic nanoparticles, such as copper (Cu) and iron (Fe). The third type of nanomaterials are carbon nanotubes (CNTs). Most researchers use commercially available nanoparticles. The typical base fluids are traditional heat transfer liquids, such as water, oil and ethylene glycol. The nanofluids using oxide and metallic nanoparticles can be synthesized using simple procedures. The general method consists of two steps; first mixing the nanoparticles into the base fluid, then applying ultrasonication. Surfactant is required for the carbon nanotube/deionized water mixture before sonication. The sonication time varies depending on the individual researcher. To characterize prepared nanofluids, researchers measure particle size with a dynamic light scattering method and utilize Scanning Electron Microscopy (SEM) or Transmission Electron Microscopy (TEM) pictures. Unfortunately, many researchers do not characterize the size distribution of the nanoparticles in suspension.

Eastman et al. (1996) prepared Cu and AI2O3 nanoparticles using the gas condensation process at the Argonne National Laboratory. They also purchased CuO and additional AI2O3 nanoparticles. They reported that AI2O3, CuO nanoparticles have such excellent dispersion properties in base fluids that no special procedures were

required to make stable nanofluids. But the Cu nanoparticle showed poor dispersion properties, when it was mixed with deionized water, it settled rapidly. TEM pictures were taken for characterization, representing considerable agglomeration among particles. The general preparation method of oxide nanofluids can be seen in Das et al. (2003)'s work. After mixing AI2O3, CuO nanoparticles with deionized water, 12 hours of sonication was applied to the mixture. They observed no sedimentation in the 12 hours subsequent to the nanofluid preparation. TEM images were also provided to observe nanoparticle shapes.

There are only a few studies on the preparation of metallic nanofluids. For example, Xuan & Li (2000) suspended Cu nanoparticles in deionized water base fluid adding 9 weight % of laurate salt as a surfactant followed by ultrasonication. The nanofluids were stable for 30 hours. TEM pictures showed some clustering. Hong et al. (2006) prepared Fe/ethylene glycol nanofluids successfully without any particular surfactant. TEM pictures revealed that Fe nanoparticles are nearly spherical and form clusters. The mean particle size was 10 nm with uniform distribution.

Special treatment is necessary to produce CNT/deionized water nanofluids. The morphology of carbon nanotubes makes the dispersion difficult. Carbon nanotubes have an extremely high aspect ratio so there is a high possibility of entanglement among nanotubes. Furthermore, the tube surfaces are attracted by strong van der Waal's forces which make dispersion challenging. The most commonly used method in the preparation of CNT/deionized water nanofluids is to add appropriate surfactant and apply ultrasonication. The role of a surfactant is to produce an efficient coating on the tube surface so that the coated tubes do not bond together. The commonly used surfactants in CNT/deionized water nanofluids are sodium dodecyl sulfate (SDS), Triton X (TX-100) and Gum Arabic (GA). GA is known as the best stabilizer among these. Ding et al. (2006) ultrasonicated CNTs first for 24 hours and dispersed the CNTs

into the deionized water/GA mixture. The TEM images show numerous carbon nanotubes have been disentangled after this process. The prepared nanofluids made in this way were found to be very stable for several months without observable sedimentation.

2.2.2 Convection of nanofiuids

In order to apply nanofluids into a cooling system, their performance in a convective heat transfer application should be confirmed. The physical effects that cause changes in thermal conductivity may be altered by the net fluid motion. Also, the nanoparticles may somehow change the fluid velocity field in natural or forced convection.

As a result, nanofluids may show unexpected heat transfer behavior other than the effect of thermal conductivity increase. However, there are only a few convection data sets for nanofluids in contrast to numerous thermal conductivity measurements for static nanofluids. So the convective heat transfer behavior of nanofluids is not well known at this time.

The investigation of nanofluid convection was initiated in 1998 by Pak & Cho (1998). They measured the αconv of 34 for AI2O3 /water nanofluids under the turbulent flow condition. They attributed the high increase in the heat transfer coefficient to the enhanced mixing caused by nanoparticles near the tube walls. In their experiment, a 10.7mm inside diameter stainless steel tube was used as a test section. The hydrodynamic entry section (x/D = 157) was long enough to accomplish fully developed flow before the heat transfer test section (x/D = 330). The tube was heated

electrically. Under a constant heat flux condition, the wall temperatures were measured by fourteen thermocouples which were attached to the outside of the tube.

Xuan & Li (2000) conducted convection experiments with Cu/water nanofluids and measured the α_{conv} of 20 under turbulent flow conditions. A brass tube of 10mm inner diameter and 800mm in length was employed as a test section. The tube was also heated electrically and eight thermocouples were installed to measure wall temperatures under a constant heat flux condition. Wen & Ding (2004) and Ding et al. (2006) investigated the convective heat transfer of Al2O3/water and CNT/water nanofluids under laminar flow conditions. They obtained αconv of up to 30 at the entrance region with Al2O3/water nanofluid and αconv of 350 with CNT/water nanofluid. They utilized a copper tube with 4.5mm inner diameter and 970mm length. The whole test section was heated by a silicon rubber flexible heater. Five thermocouples were mounted on the test section to measure wall temperature distribution. Their results of huge αconv values, however, are unconvincing because their plain water measurements show up to 30% discrepancy with known values.

Lee & Mudawar (2007) measured the α_{conv} of 2.3 with Al_2O_3/water nanofluid in laminar flow in 21 parallel rectangular microchannels which were milled into a copper block. Each microchannel was 215μm wide by 821μm deep. Heating was supplied by 12 cartridge heaters on the bottom of the copper block. Four thermocouples were inserted in the copper block near the microchannels and provided the temperature measurements.

Heris et al. (2006) measured α_{conv} of 15 with Al_2O_3/water nanofluid for laminar flow in a tube. The test section consisted of a 6mm diameter inner copper tube and 32mm diameter outer stainless steel tube. Nanofluids flowed inside the inner tube while saturated steam entered the annular section, which made constant wall temperature

condition. Two thermocouples were installed at the inlet and outlet for measuring bulk temperature of the fluids. Table 2.1 shows the summary of the past nanofluid convection data. Similar to the conduction data, there is a large variation of data. The α_{conv} of $A1_20_3$/water nanofluid varies from 2.3 to 30 under laminar flow condition. Due to the insufficient data, no firm conclusions can be made.

Table 2.1: The α_{conv} of nanofluids

Particle material	Particle size (nm)	Basefluid material	α_{cond}	Hydraulic dia. Of tube (mm)	Flow condition	References
Al_2O_3	13	water	34	10.7	Turbulence	(Pak & Cho, 1998)
Al_2O_3	27-56	water	30	4.5	Laminar	(Wen & Ding, 2004b)
Al_2O_3	36	water	2.3	0.7	Laminar	(Lee & Mudawar, 2007)
Al_2O_3	20	water	15	6	Laminar	(Heris et al., 2006)
Cu	100	water	20	10	Turbulence	(Xuan& Li, 2000)
CNT	Not reported	water	350	4.5	Laminar	(Ding et al., 2006)

2.2.3 Viscosity of nanofluids

Since viscosity of fluids determines the required pumping power in heat transfer systems, viscosity change of nanofluids should be investigated very carefully to assess the efficiency of nanofluids. However, little effort has been devoted to the viscosity of nanofluids and there are inconsistencies in the available data. More studies are required to understand the effect of nanoparticles on viscosity. The viscosity of nanofluids has been measured by either measuring pressure drop in a tube or using a viscometer. Table

2.2 shows the summary of previous viscosity measurements. Based on the available viscosity data, some trends were found.

The viscosity of nanofluids generally increased exponentially as a function of volume concentration. Because the viscosity increase is nonlinear, the αvisc value is different for each volume concentration of the same nanofluid. Also, viscosity of the nanofluid decreased with increasing temperature similar to the plain base fluids. Most of the researchers agreed that the viscosity of nanofluids is apparently higher than the traditional viscosity model of particle laden fluid such as the Einstein model or Batchelor's model. However, there is an inconsistency whether nanofluids are Newtonian or Non-Newtonian fluid. Some researchers found that nanofluids have shear-thinning behavior which means the viscosity decrease as the shear-rate increases. Others describe nanofluids as Newtonian fluid. Sufficient data should be provided to clarify the nanofluid behavior.

Wang et al. (1999) measured the viscosity of Al_2O_3/water nanofluids prepared by three different methods and concluded that the preparation method affects the viscosity of nanofluids. They claimed that the viscosity increases less as the nanoparticles in the fluids are well dispersed. In shear rate-controlled measurements, a constant rotation speed is maintained and the resulting torque generated by the sample is determined using a suitable stress-sensing device, such as a torsion spring or strain gauge.

Kwak & Kim (2005) conducted viscosity measurement of CuO/ethylene glycol nanofluid with a ARES-LS (TA instruments) rotational viscometer, which measures the applied torque on the sample while maintaining a selected shear rate. They found that the nanofluid has a shear-thinning behavior. The αvisc values of nanofluids decreased significantly from 100 to 0 with shear rate increase. They attributed the results to the

rodlike particle shape caused by particle aggregation. On the contrary, Chevalier et al. (2007) carried out viscosity measurements of Silica/Alcohol nanofluids and observed Newtonian behavior over a broad range of shear rates. Additionally, they observed nanofluid viscosity increase with particle size decrease. Tseng & Wu (2002) measured viscosity of Al2O3/water nanofluid and observed transition from shear thinning to shear thickening when the shear rate exceeds a critical level.

Prasher et al. (2006c) performed viscosity experiments with Al203/Propylene Glycol (PG). Their results showed that the viscosity of nanofluid was constant over a wide range of shear rate and the viscosity was much higher than Einstein's model. They proposed particle aggregation to explain this unexpected high viscosity. They also conducted analysis about the nanofluid efficiency and concluded that the viscosity has to be increased by more than a factor of 4 to make the nanofluid thermal performance worse than that of the base fluid.

Xuan k Li (2000) reported no viscosity increase of Cu/water nanofluid. They measured the pressure drop of Cu/water nanofluid in a 10mm diameter by 800mm long tube. Pak k Cho (1998) measured the pressure drops of A1203/water nanofluid in the rectangular 215/um wide by 821//m deep microchannel and acquired αvisc of from 0 to 19 depending on the Reynolds number from 200 to 800.

Table 2.2: The α_{visc} of various nanofluids

Particle material	Particle size (nm)	Base fluid material	α_{visc}	Measurement technique	References
Al_2O_3	28	Water	10	Viscometer	(Wang et al., 1999)
Al_2O_3	13	Water	0-20	Viscometer	(Pak & Cho, 1998)
Al_2O_3	36	Water	0-19	Pressure drop	(Lee & Mudawar, 2007)
Al_2O_3	37	Water	0-100	Viscometer	(Tseng & wu, 2002)
Al_2O_3	28	Ethylene	7.6	Viscometer	(Wang et al., 1999)

		glycol			
Al_2O_3	40	Propylene glycol	14	Viscometer	(Prasher et al., 2006c)
CuO	12	Ethylene glycol	0-100	Viscometer	(Kwak & Kim, 2005)
CuO	100-200	Ethylene glycol	10	Viscometer	(Liu et al., 2006)
TiO_2	7-20	Water	20-100	Viscometer	(Tseng & lin, 2003)
TiO_2	27	Water	0.4	Viscometer	(Pak & cho, 1998)
TiO_2	25	Ethylene glycol	13	Viscometer	(Chen et al., 2007)
Cu	100	Water	0	Pressure drop	(Xuan & Li, 2000)
CNT	Not reported	Water	0.2 x 10^7	Viscometer	(Ding et al., 2006)
Silica	35	Alcohol	10-14	Viscometer	(Chevalier et al., 2007)
Silica	94	Alcohol	5-8	Viscometer	(Chevalier et al., 2007)
Silica	190	Alcohol	5-6	Viscometer	(Chevalier et al., 2007)

2.2.4 Heat Transfer Variables in Nanofluids

The heat transfer enhancement in nanofluids has been attributed to many mechanisms, and each will be discussed individually. As the reader will see, most research has been done on how variables affect the effective thermal conductivity, not the heat transfer coefficient independently.

1) Particle Agglomeration

One challenge with nanofluids is that the nanoparticles tend to agglomerate due to molecular forces such as Van Der Waals force. Karthikeyan, Philip, and Raj found in their experiments with copper oxide/water nanofluid that the nanoparticle size and cluster size have a significant influence on thermal conductivity. They also found that

agglomeration is time-dependent. As time elapsed in their experiment, agglomeration increased, which decreased the thermal conductivity. Figure 2.3 shows how the thermal conductivity decreases with time. From Figure 2.3, it can be seen that the thermal conductivity of the nanofluids drops dramatically as time increases, which Karthikeyan, Philip, and Raj attribute to particle agglomeration. They confirmed this theory microscopically, which is shown in Figure 2.4.

As one can see in the Figure 2.4, the clustering of the nanoparticles greatly increases with time, and it is noticeable after only 60 minutes. Karthikeyan, Philip, and Raj observed that there was no sedimentation when the photos were taken. Agglomeration causes the effective surface area to volume ratio of the nanoparticles to decrease, which reduces the thermal conductivity of the fluid. The group also concluded that agglomeration increases with increasing nanoparticle concentration because the particles are closer together and experience more Van Der Waals attraction. Wang measured the viscosity of alumina-water nanofluid and found that viscosity increases as nanoparticles agglomerate, which could also contribute to the lower thermal conductivity when agglomeration increases.

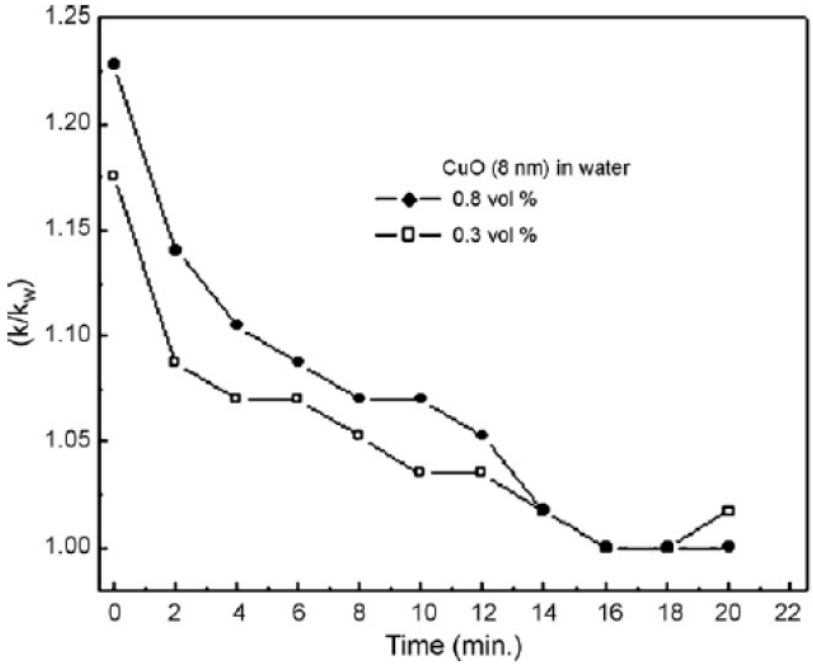

Figure 2.3: Thermal conductivity decreases with time (Karthikeyan, N. R., J. Philip, et al., 2008)

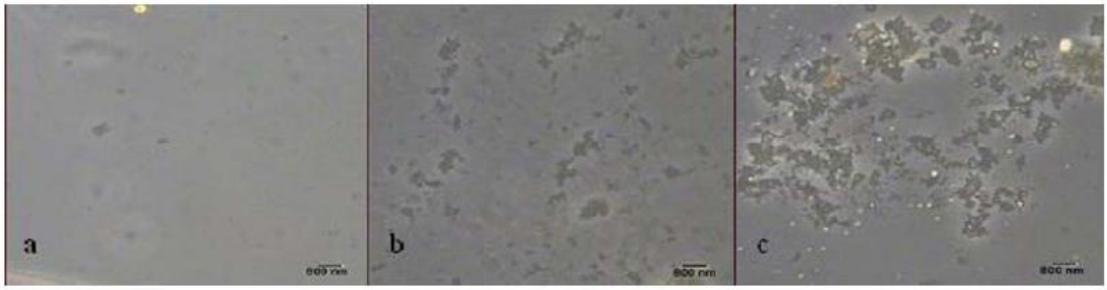

Figure 2.4: 0.1% volume fraction of copper oxide nanoparticles in water after (Karthikeyan, N. R., J. Philip, et al., 2008)

a) 20 minutes b) 60 minutes c) 70 minutes.

2) Volume Fraction

Effective thermal conductivity of nanofluid increases with increasing volume fraction of nanoparticles, but as the volume fraction of nanoparticles increases, it may no longer be valid to assume that the nanoparticles stay suspended. This is why it is more effective to use a very small volume fraction in nanofluids.

3) Brownian Motion

Several researchers have found that Brownian motion, which is the random movement of particles, is one of the key heat transfer mechanisms in nanofluids. It is thought to cause a microconvection effect. Brownian motion only exists when the particles in the fluid are extremely small, and as the size of the particles gets larger, Brownian motion effects diminish.

4) Thermophoresis

Thermophoresis occurs because of kinetic theory in which high energy molecules in a warmer region of liquid impinge on the molecules with greater momentum than molecules from a cold region. This leads to a migration of particles in the direction opposite the temperature gradient, from warmer areas to cooler areas.

5) Nanoparticle size

Several studies have found that as nanoparticles are reduced in size, the effective thermal conductivity of the nanofluid increases. This is because of two reasons. As the nanoparticle size is reduced, Brownian motion is induced. Also, lighter and smaller nanoparticles are better at resisting sedimentation, one of the biggest technical challenges in experimenting with nanofluids.

6) Particle shape/surface area

Several studies have found that rod-shaped nanoparticles, such as carbon nanotubes, remove more heat than spherical nanoparticles. This may be due to the fact that rod-shaped particles have a larger aspect ratio (the ratio between a particle's surface area to volume) than spherical nanoparticles.

7) Liquid layering on the nanoparticle-liquid interface

Some researchers have suggested that there is liquid layering on the nanoparticles, which helps enhance the heat transfer properties of the nanofluid. The thickness and thermal conductivity of the nanolayer are not known yet, but the liquid molecules close to a solid surface have been proven by Yu, Richter et. al., (2000) to form layers. Ren, Xie, and Cai (2005) made a theoretical model to study the change in thermal conductivity from adding liquid layering on the nanoparticles. They assumed

that the thermal conductivity of the layer would be somewhere between the thermal conductivity of the bulk fluid and the nanoparticle. They found that an increase in the layer thickness leads to a large thermal conductivity enhancement. Their results are shown in Figure 2.5.

In the figure 2.5, *d* is the thickness of the liquid layering, and rp is the nanoparticle radius. As one can see, the thermal conductivity of the nanofluid goes up with increasing surface layering. Ren, Xie, and Cai also found that as the nanoparticles increased in size, the effects of the liquid layering became weaker.

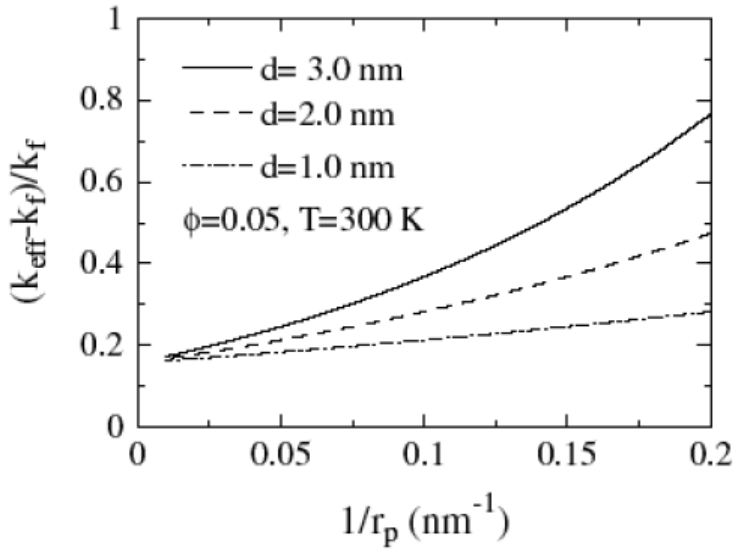

Figure 2.5: Dependence of thermal conductivity enhancement on the reciprocal of the nanoparticle radius (Ren, Y., H. Xie, et al., 2005).

8) Temperature

Nanofluids' effective thermal conductivity and Brownian motion increase with temperature. Chon, Kihm, Lee and Choi did an experimental investigation of alumina nanofluids and how their thermal conductivity varies with temperature. Figure 2.6 shows their results. From Figure 2.6, it is evident that the normalized thermal conductivity, or the ratio of the thermal conductivity of the nanofluid to the thermal conductivity of the base fluid, is highly dependent upon temperature as well as volume fraction of nanoparticles. As the temperature and volume fraction of nanoparticles increase, the thermal conductivity increases as well.

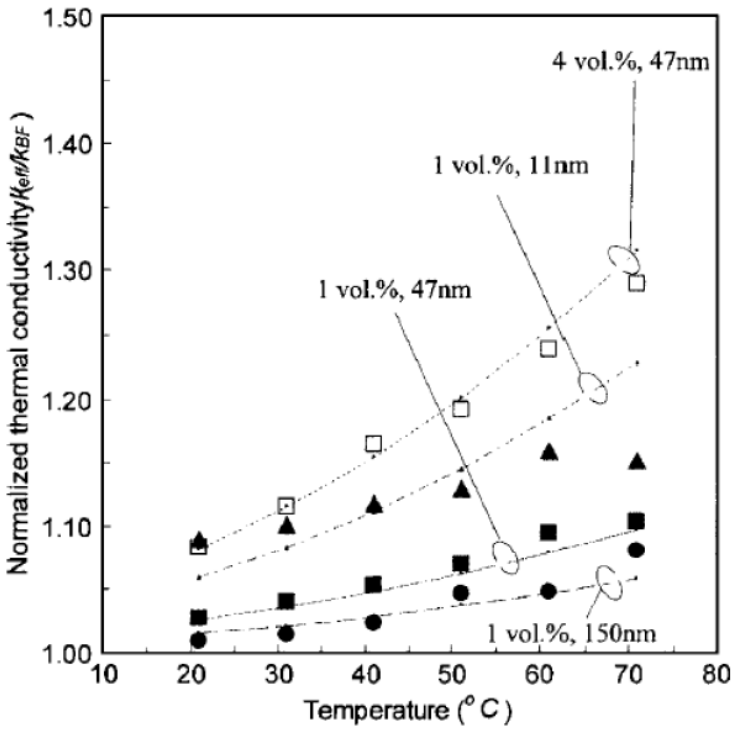

Fig. 2.6: Experimental results of thermal conductivity dependence on temperature (Chon, C. H., K. D. Kihm, et al., 2005)

9) Reduction in thermal boundary layer thickness.

Several researchers have mentioned that a reduction in the thermal boundary layer thickness may be a mechanism that causes heat transfer enhancements in nanofluids, but there has been very little research in the area to date.

Research with nanofluids is still fairly new, so some of the mechanisms that affect heat transport in nanofluid have yet to be studied in depth. In addition, most research has been done on mechanisms that affect thermal conductivity and not as much research has been done on mechanisms that affect the heat transfer coefficient in convection.

CHAPTER 3

Methodology

3.1 Work breakdown Structures

Work breakdown structure is a management tool to break a project down into manageable pieces and to ensure that all of the work elements needed to complete the research work scopes is identified. In this study, the works are divided into 5 main categories: Literature review, thermophysical properties of nanofluid and air, mathematical formulation of electric motors, analysis and report writing. The objectives of study are achieved when all of the activities in each level are accomplished. Figure 3.1 shows the work break down structure used in this study

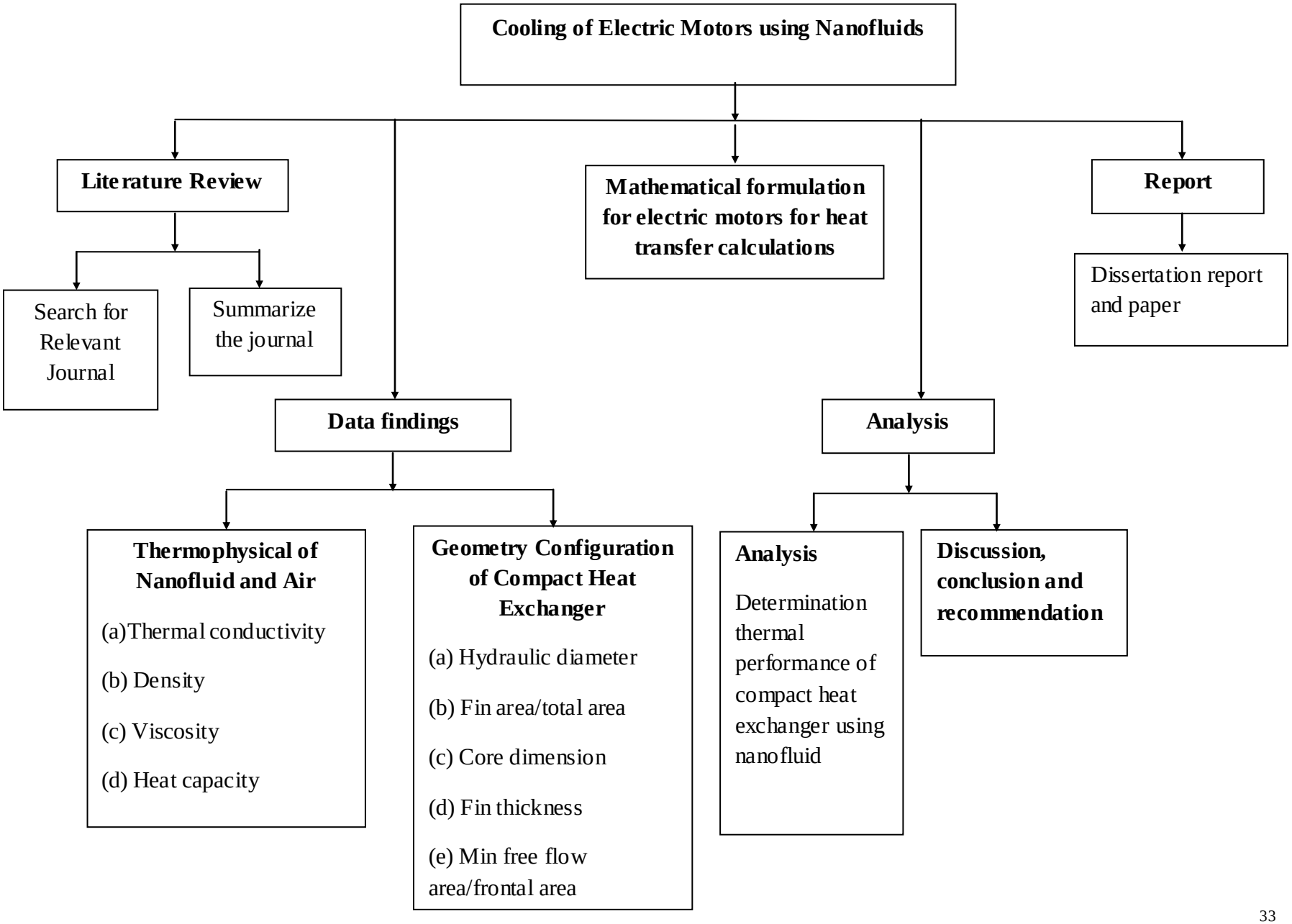

Figure 3.1 Work breakdowns Structure

3.2 Input Data

3.2.1 Thermophysical Properties of Coolants and Air

Among the many types of nanofluids, ethylene glycol-based aluminum oxide (Al_2O_3) nanofluid is only considered in this study. Several thermophysical properties of the nanofluid are needed in this study. They are specific heat, density, thermal conductivity, viscosity and Prandtl number. Properties for the coolant and air are obtained from the literatures as shown in Table 3.1 and Table 3.2. These properties are based on temperature at 360K for coolant while 311K is for air. Temperature of coolant must be higher than the air because the heat is transferred from coolant to air. It is obtained from average operating temperature value from literature. Another important parameter is thermal conductivity of fin material (copper). Its thermal conductivity is 398W/mK at 334K based on average operating temperature of air and coolant.

Table 3.1 Thermophysical Properties of Coolant and Aluminum oxide Particles (Incopera *et al.*, 2007)

Property	Ethylene Glycol (360K)	Aluminum oxide (360K)
Specific heat(J/kgK)	2682	870.0
Density(kg/m3)	1071	3970
Thermal Conductivity(W/mK)	0.2622	37.84
Viscosity (Ns/m2)	0.003066	

Table 3.2 : Thermal Properties of Air (Incopera *et al*., 2007)

Property	At 311 K
Viscosity(Ns/m2)	0.00001898
C_p(J/kg.K)	1007.4
Prandlt number	0.706

For nanofluid, these properties are calculated from formula obtained in literatures as shown in Table 3.3. Thermal conductivity of the calculated values is compared with the relevant literature since theoretical values usually give lower thermal conductivity. In this study, the thermal conductivity values from Eastman, et al (2001), were used in calculating thermal performances.

Table 3.3: Theoretical Formula to Calculate Heat Transfer Properties of Ethylene Glycol-based Aluminum oxide Nanofluid

No	Properties	Formula	Reference
1	Heat Capacity	$C_{nf}=\frac{(1-\varphi)\rho_f C_f+\varphi\rho_p C_p}{\rho_{nf}}$	Velagapudi, *et al.*, (2008)
2	Density	$\rho_{nf}=(1-\varphi)\rho_f+\varphi\rho_p$	
3	Viscosity	$\mu_{nf}=\mu_f\frac{1}{(1-\varphi)^{2.5}}$	Lee *et al.*,2008
4	Thermal Conductivity	$k=k_f\left[\frac{k_p+(n-1)k_f-(n-1)\varphi(k_f-k_p)}{k_p+(n-1)k_f+\varphi(k_f-k_p)}\right]$	Eastman, *et al.* (2001)

3.2.2 Geometry Configuration of Compact Heat Exchanger

Several geometry configuration and operating conditions are required in this study. These data are obtained from literatures as shown in Table 3.4 and Table 3.5

Table 3.4 : Core Geometry of Flat Tubes, continuous fins and Operating Condition of Compact Heat Exchanger (Vasu *et al*., 2008)

Num	Description	Air	Coolant
1	Fluid inlet temperature	20-55^{o}C (Assume T_a= 37.5^{o}C	70-95^{o}C (Assume T_c=86.5^{o}C)
2	Core width	600 mm	
3	Core height	500 mm	
4	Core depth	400 mm	
5	Tube Size	(18.72 x 2.45) mm	

Table 3.5: 11.32-0.737-SR Surface Characteristic of Compact Heat Exchanger (Kays & London, 1984)

Num	Description	Air Side	Coolant side
1	Tube arrangement	Staggered	
2	Fin type	Ruffled	
3	Fin pitch	4.46 fin/cm	
4	Fin thickness	0.01cm	
5	Hydraulic diameter, D^h	0.351cm	0.373cm
6	Free flow area/frontal area, σ	0.78	0.129
7	Heat transfer area/total volume,α	$886 m^2/m^3$	$138 m^2/m^3$
8	Fin area/total area,β	0.845	

3.3 Mathematical Formulation of Ethylene Glycol Based Aluminum Oxide Nanofluid in Electric Motors Cooling

The mathematical formulations can be divided into two sections which are air side and nanofluid side. Figure 3.2 depicts a typical compact heat exchanger that commonly used in industries.

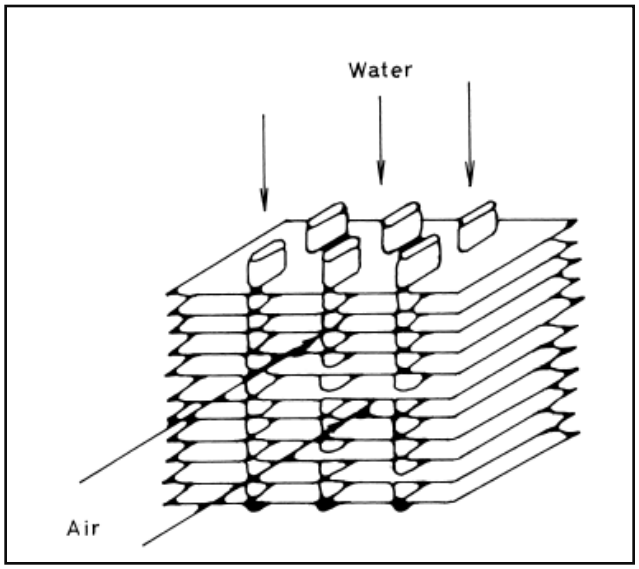

Figure 3.2: Typical Flat Tubes, Continuous Fin Compact Heat Exchanger(Kays & London, 1984)

3.3.1 Air Side Calculation (Kays & London, 1984) and (Vasu *et al.*, 2008)

The following equations (air side and nanofluid side) were used to calculate the properties of air and nanofluid where the heat is exchanged from fluid to air. So, both air side and nanofluids side calculations are important to calculate heat exchanger effectiveness (NTU), overall heat transfer coefficient and finally the total heat transfer rate for the system.

`

(a) Air heat capacity rate, C_a

$$C_a = W_a C_{p,a} \tag{3.1}$$

(b) Heat transfer coefficient, h_a

$$h_a = \frac{j_a G_a C_{p,a}}{Pr_a^{2/3}} \tag{3.2}$$

where

$$j_a = \frac{0.174}{Re_a^{0.383}} \tag{3.3}$$

$$G_a = \frac{W}{A_{fr}\sigma_a} \tag{3.4}$$

$$Re_a = \frac{G_a D_{h,a}}{\mu_a} \tag{3.5}$$

(c) Fin efficiency of plate fin, η_f

$$\eta = \frac{\tanh mL}{mL} \tag{3.6}$$

where

$$m = \sqrt{\frac{2h_a}{kt}} \tag{3.7}$$

(*d) Total surface temperature effectiveness,*

$$\eta_0 = 1.0 - (1.0 - \eta_f) \times \frac{A_f}{A} \tag{3.8}$$

3.3.2 Nanofluid Side Calculation

(a) Heat transfer Coefficient

$$h_{nf}=\frac{Nu_{nf}\,k_{nf}}{D_{h,nf}} \tag{3.9}$$

where

$$Nu_{nf} = 0.023Re_{nf}^{0.8}Pr_{nf}^{0.3} \tag{3.10}$$

$$Re_{nf}=\frac{G_{nf}D_{h,nf}}{\mu_{nf}} \tag{3.11}$$

$$\mu_{nf}=\mu_f\frac{1}{(1-\varphi)^{2.5}} \tag{3.12}$$

$$G_{nf} = \frac{W_{nf}}{A_{fr}\,\sigma_{nf}} \tag{3.13}$$

$$v_{nf}=\frac{W_{nf}}{\rho_{nf}} \tag{3.14}$$

$$Pr_{nf}=\frac{\mu_{nf}C_{p,nf}}{k_{nf}} \tag{3.15}$$

$$c_{p,nf} =\frac{(1-\varphi)\rho_f C_{p,f}+\varphi\rho_p C_{p,p}}{\rho_{nf}} \tag{3.16}$$

$$\rho_{nf}=(1-\varphi)\rho_f+\varphi\rho_p \tag{3.17}$$

(b) Heat capacity rate, C_{nf}

$$C_{nf}=W_{nf}C_{p,nf} \tag{3.18}$$

(c) Heat Exchanger effectiveness for cross flow unmixed fluid, ε

$$\varepsilon=1-\exp\left[\left(\frac{1}{C^*}\right)\right](NTU)^{0.22}\left\{\exp\left[-C^*(NTU)^{0.78}\right]-1\right\} \tag{3.19}$$

where

$$C^*=\frac{C_{minimun}}{C_{maximum}} \tag{3.20}$$

$$NTU=\frac{U_a A_{fr,a}}{C_a} \tag{3.21}$$

(d) Overall heat transfer coefficient, based on air side

Neglecting wall resistance and fouling factor

$$\frac{1}{U_a}=\frac{1}{\eta_o h_a}+\frac{1}{\left(\frac{\alpha_{nf}}{\alpha_a}\right)h_{nf}} \tag{3.22}$$

(e) Total heat transfer rate

$$Q = \varepsilon C_{min}(T_{nf,in} - T_{a,in}) \tag{3.23}$$

3.4 Analysis

This study is concentrate on total heat transfer which can be achieved when aluminum oxide nanoparticles were mixed in ethylene glycol basefluid. To find the outcome, Ms Excel was used to analyze thermal performance of compact heat exchanger. Mathematical formulation for compact heat exchanger, nanofluid and relevant input data from previous section were used in this study. Analysis was done based on the following:

(a) Thermo physical properties of coolant (ethylene glycol + aluminum oxide).

(b) Influence of volume fraction of aluminum oxide particles to the thermal performance of electric motors (heat transfer rate, Q)

3.5 Flow Chart

The following flow chart indicating the flows of processes which were carried out throughout this study until the end (final preparation of the dissertation).

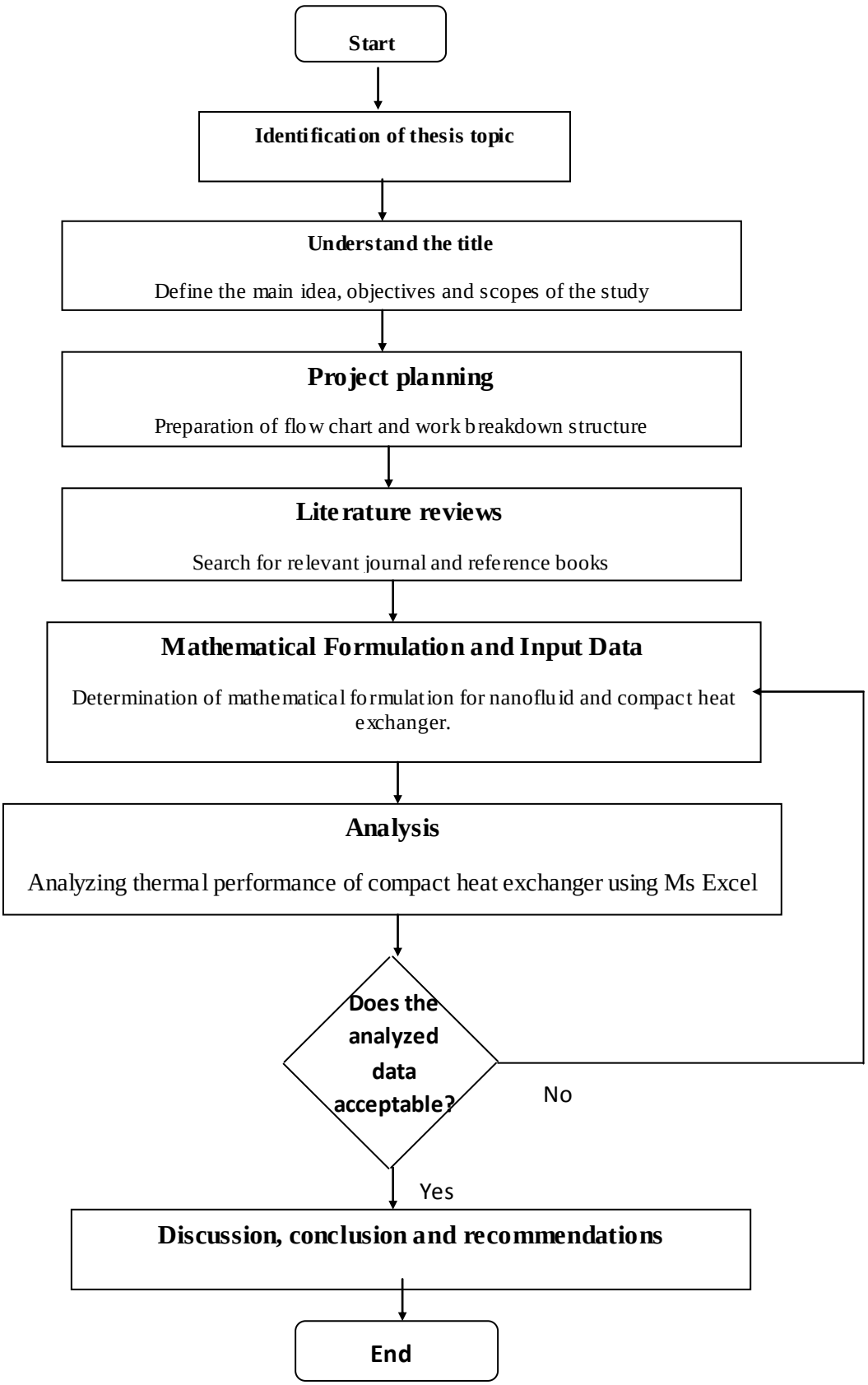

Figure 3.3 Flow Chart

CHAPTER 4

Results and Discussion

This chapter reviews the result and discussion obtained from this study. Section 4.1 reviews discussion on thermophysical properties of coolants while influence of volume fraction of aluminum oxide particles to thermal performance of electric motors in section 4.2.

4.1 Thermophysical Properties of Coolant

The finding indicates that thermophysical properties of ethylene glycol coolant change with addition of aluminum oxide particles. Using equations listed in Table 3.3, the thermo physical properties of nanofluid are calculated and plotted in relation of aluminum oxide volume fraction. Density and viscosity of ethylene glycol coolant increase with addition of aluminum oxide particles as shown in Figure 4.1 and 4.2 respectively. At 2% volume fraction of aluminum oxide particles, the ethylene glycol coolant exhibits 5.41% increase for density and 5.19% increase for viscosity. As for specific heat, it will be lowered with addition of aluminum oxide particles as shown in

Figure 4.3. For instance, specific heat of ethylene glycol decreases 4.75% at 2% volume fraction of aluminum oxide. Therefore, less energy per unit mass is needed to increase its temperature by one degree Celsius. This clearly shows that volume fraction of aluminum oxide particles play major effect on these properties.

Thermal conductivity of ethylene glycol coolant also increases with aluminum oxide particles as depicted in Figure 4.4. In this study, the set of data obtained from Eastman, *et al.,* (2001) were considered and it shows that by addition of 2% aluminum particles, it can increase the thermal conductivity up to 6%. From the study, it is noted that small addition of particles is enough to provide higher thermal conductivity. Therefore, it can minimize the clogging problems when it applied.

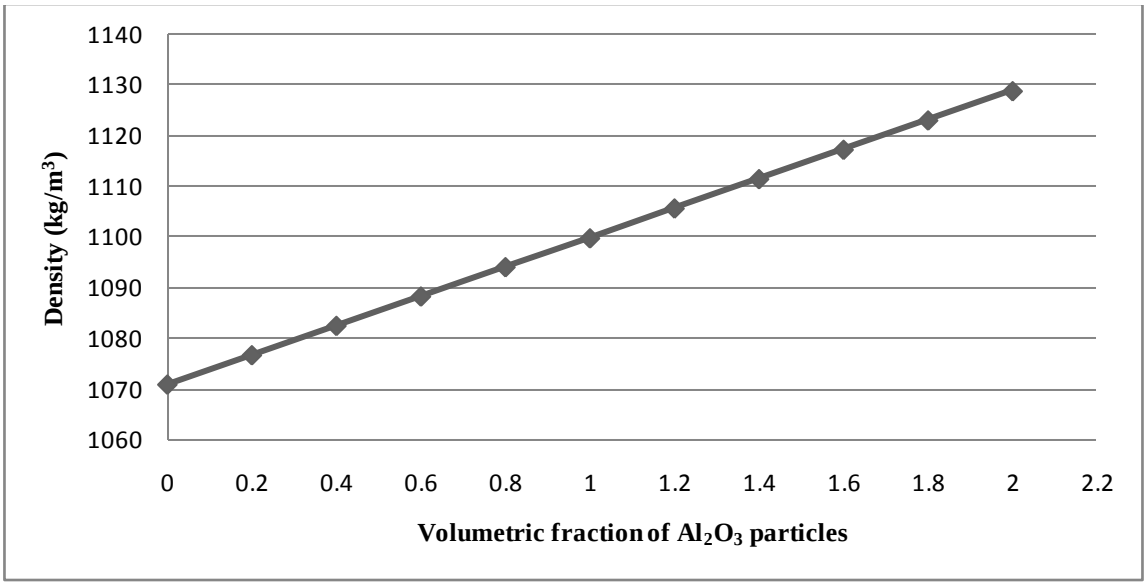

Figure 4.1: Effect of Volume Fraction of Aluminum Oxide Particles to Density of Ethylene Glycol

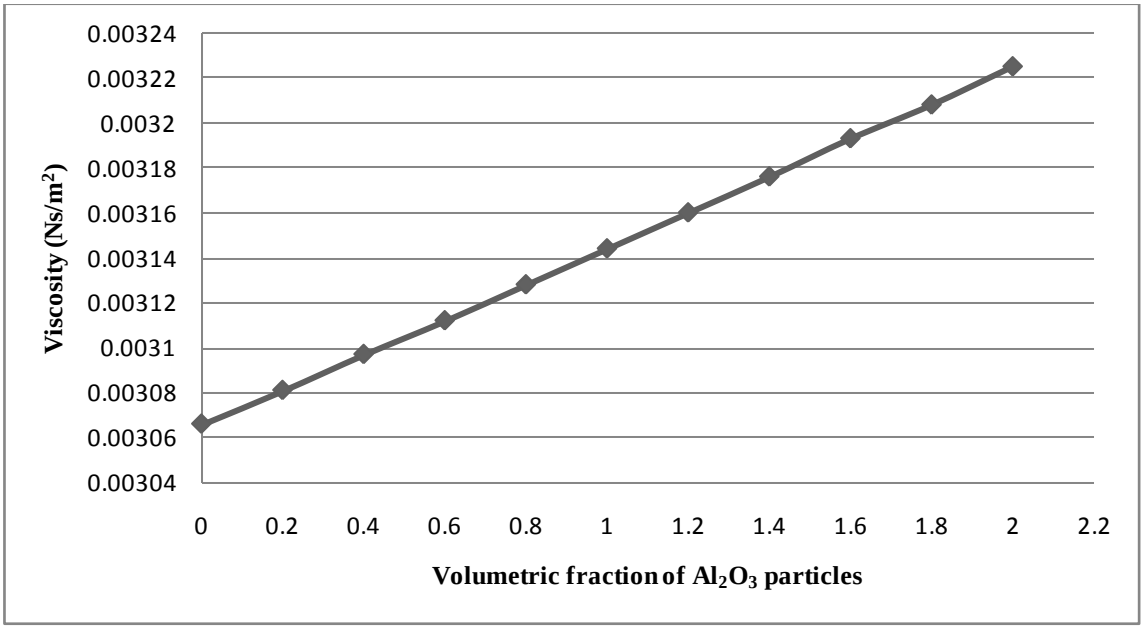

Figure 4.2: Effect of Volume Fraction of Aluminum Oxide Particles to Viscosity of Ethylene Glycol

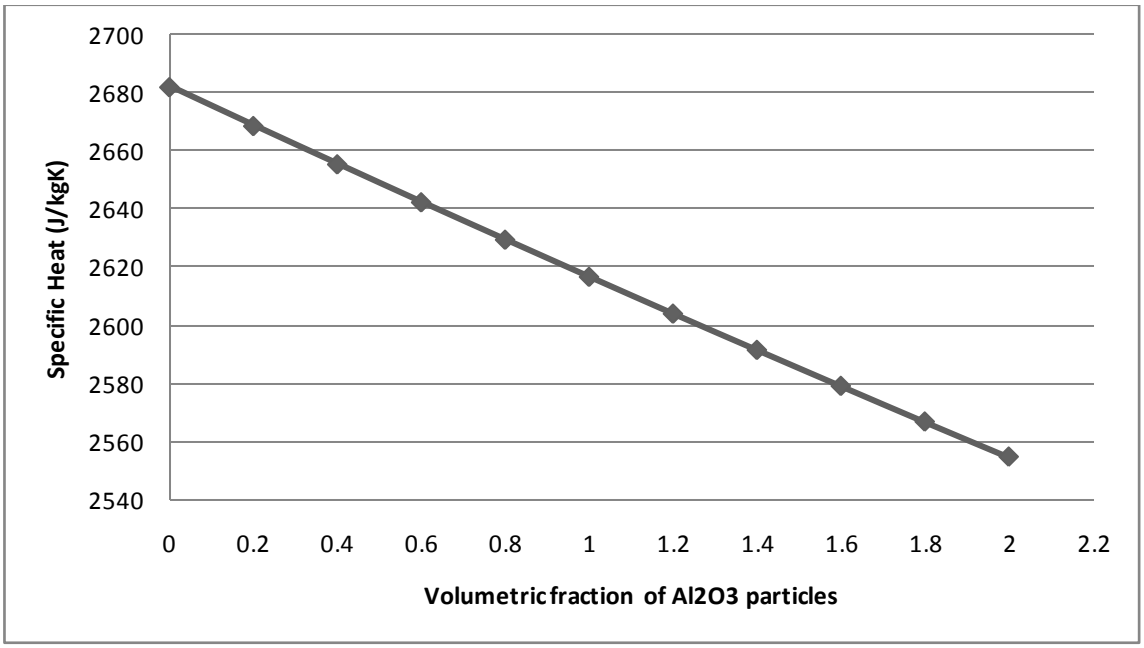

Figure 4.3: Effect of Volume Fraction of Aluminum Oxide Particles on Specific Heat of Ethylene Glycol

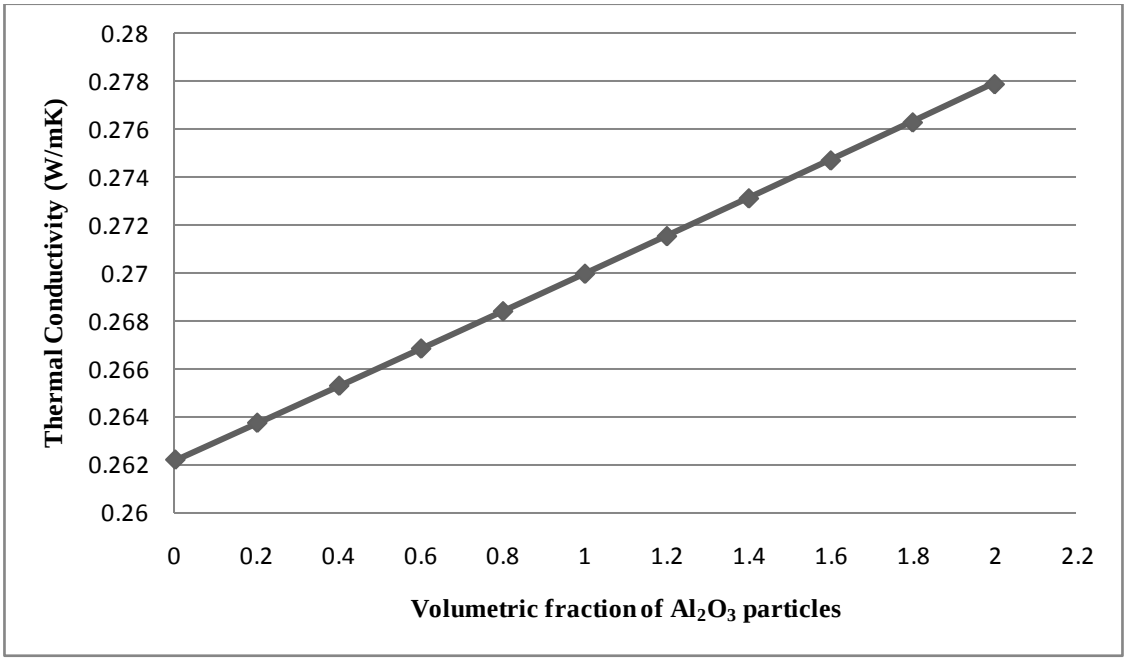

Figure 4.4: Effect of Volume Fraction of Aluminum Oxide Particles on Thermal Conductivity of Ethylene Glycol

4.2 Influence of Volume Fraction of Aluminum Oxide Particles to Thermal Performance of Electric Motors

This section analyses the thermal performance of electric motors at fixed air (4000) and coolant (5000) Reynold number. Figure 4.5 depicts that as aluminum oxide volume fraction increases, the coolant mass flow rate increases as calculated based on equation 3.11 and 3.13.This is mainly due to an increase in viscosity level of nanofluid. From Figure 4.6, it can be observed that coolant volumetric flow rate decreases with aluminum oxide volume fraction. At 2.0% aluminum oxide volume fraction, the coolant volumetric flow rate reduced 0.22% compared to basefluid. Prandtl number of the coolant is dependent on viscosity, thermal conductivity and specific heat. In this study, it is found that Prandtl number of coolant decreases with aluminum oxide particles

which is mainly due to higher thermal conductivity of nanofluid. This is shown in Figure 4.7. Since there is no specific empirical formulation for ethylene-glycol based aluminum oxide nanofluid, Dittus-Boelter equation is used to calculate Nusselt number for both types of coolants. The results are then plotted as shown in Figure 4.8 which indicates lower coolant Nusselt number with addition of aluminum oxide particles. Its shows that Nusselt number decrease 1.68% when aluminum oxide at 2% of volume fraction.

Ethylene glycol based aluminum oxide nanofluid demonstrates higher coolant heat transfer coefficient and overall heat transfer coefficient based on air side as shown in Figure 4.9 and 4.10. Heat transfer coefficient of coolant increases linearly with aluminum oxide particles. 4.21% enhancement can be achieved at 2% volume fraction of aluminum oxide particles. Overall heat transfer coefficient based on air side also increases with aluminum oxide particles. It can be translated to reduction of air side area up to 0.9% at 2% aluminum oxide particles. Kulkarni *et al.*, (2009) in their investigation of nanofluid application in building heating also reveal possibility reduction of heat transfer surface area of heat exchanger. It is found that 20.37%, 17.3% and 8.5% area reduction for 6% Aluminum Oxide oxide, 6% aluminum oxide and 6% silicon carbide of EG/water basefluid respectively. As the volume fraction of nanofluid increases, the heat transfer rate increased up to 0.15% at 2% volume fraction of aluminum oxide particles as shown in Figure 4.11. The heat transfer rate is calculated based equation 3.26.

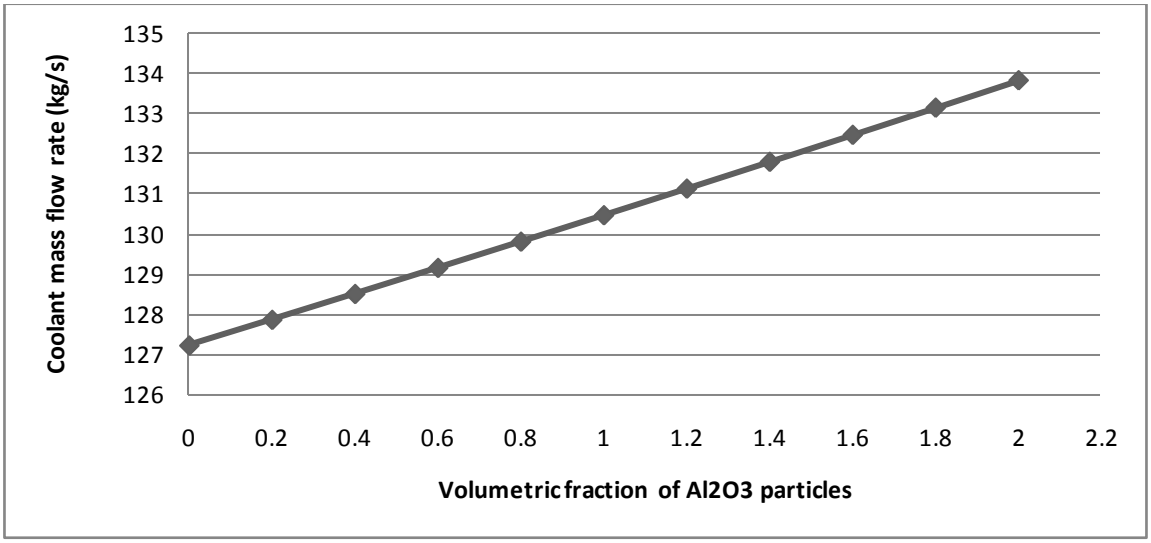

Figure 4.5: Effect of Aluminum Oxide Volume Fraction to Coolant Mass Flow Rate at Constant Air and Coolant Reynold Number

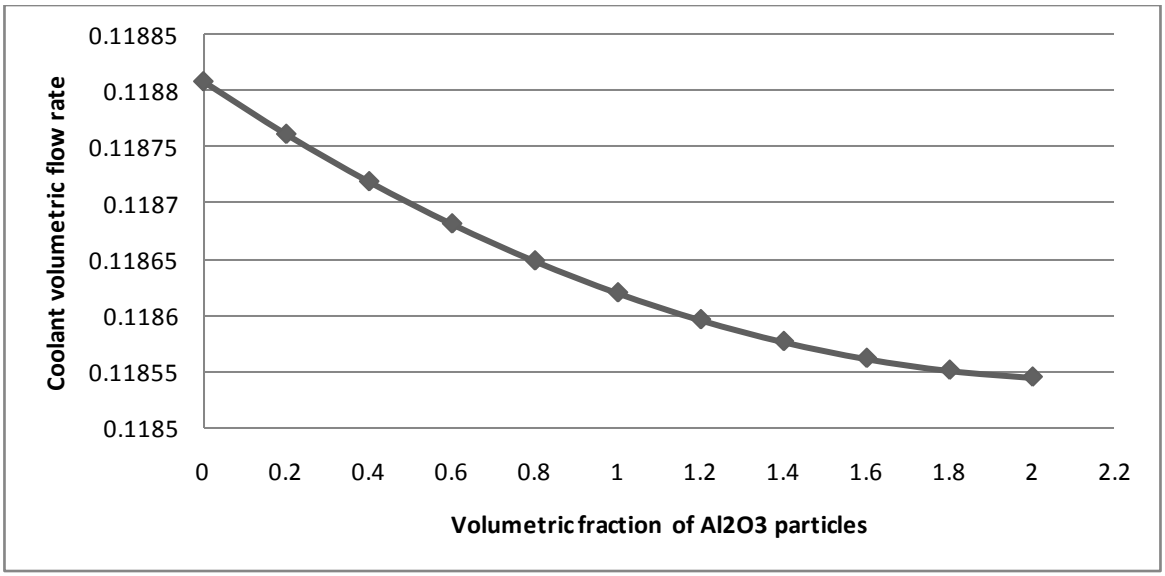

Figure 4.6: Effect of Aluminum Oxide Volume Fraction to Coolant Volumetric Rate at Constant Air and Coolant Reynold Number

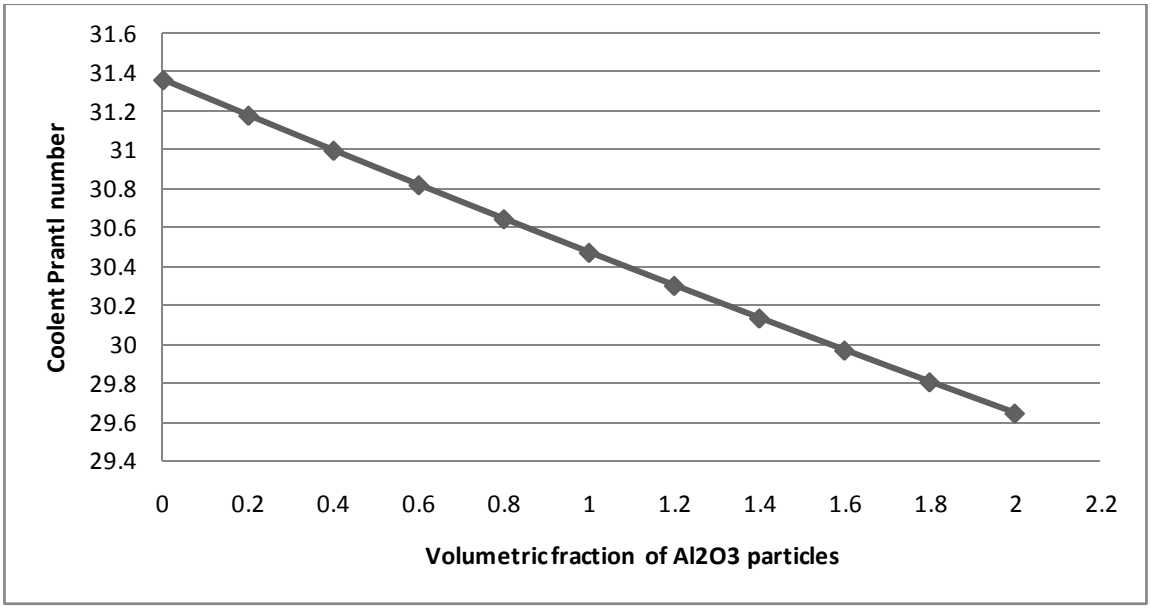

Figure 4.7: Effect of Aluminum Oxide Volume Fraction to Coolant Prandtl at Constant Air and Coolant Reynold Number

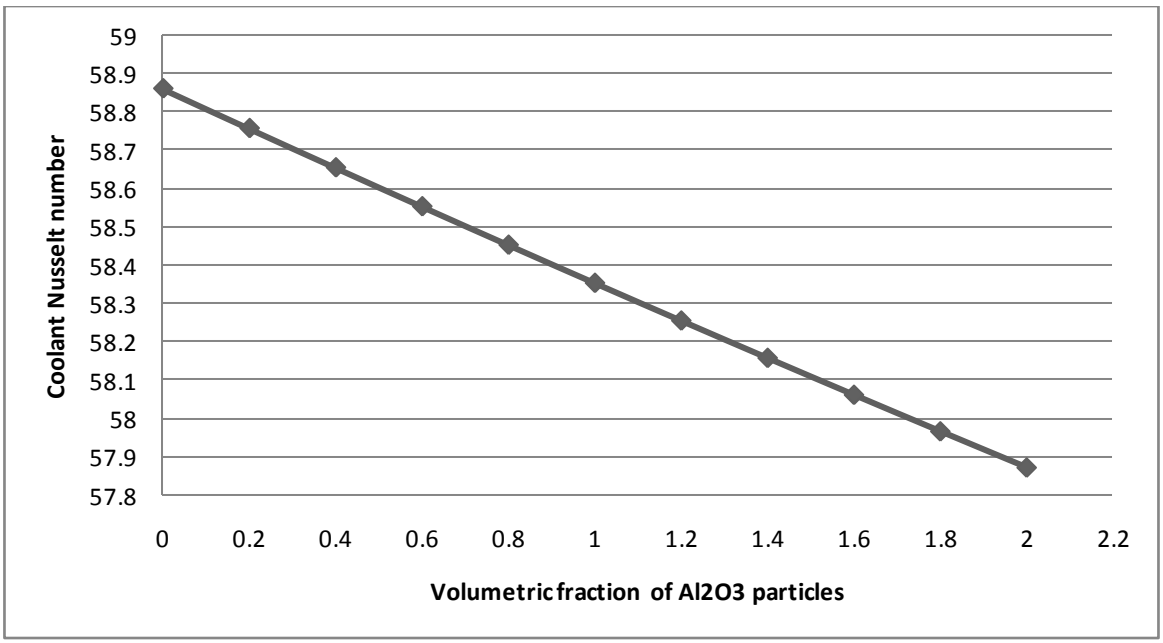

Figure 4.8: Effect of Aluminum Oxide Volume Fraction to Coolant Nusset Number at Constant Air and Coolant Reynold Number

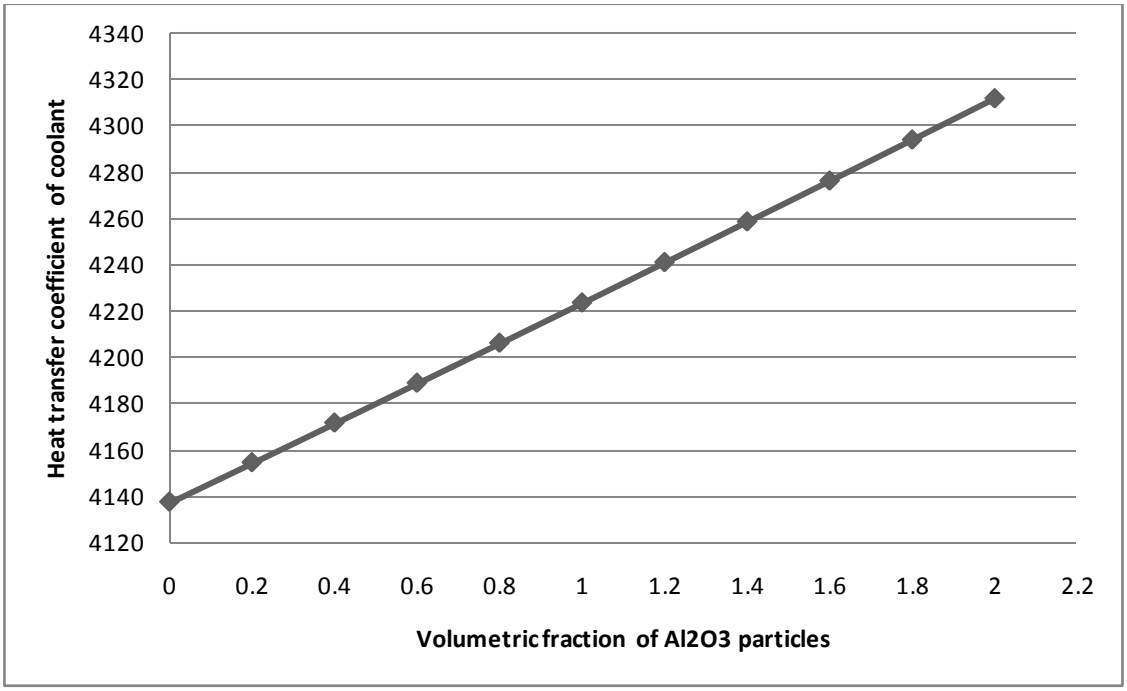

Figure 4.9: Effect of Aluminum Oxide Volume Fraction to Heat Transfer Coefficient of Coolant at Constant Air and Coolant Reynold Number

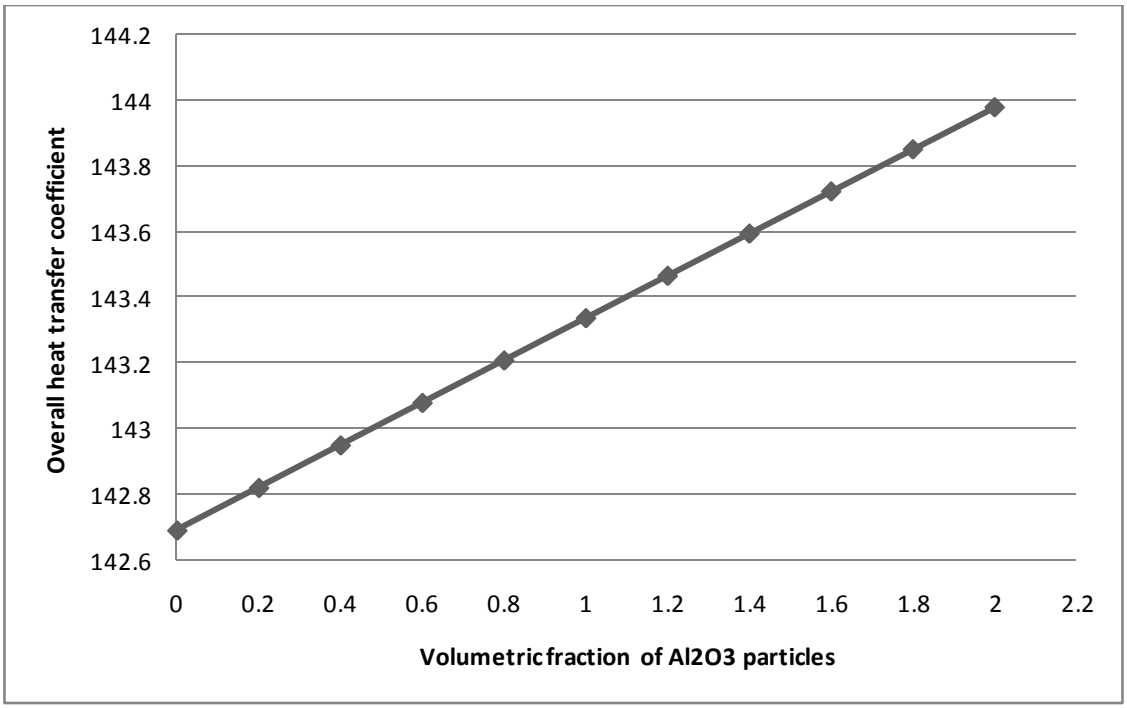

Figure 4.10: Effect of Aluminum Oxide Volume Fraction to Overall Heat Transfer Coefficient based on Air side at Constant Air and Coolant Reynold Number

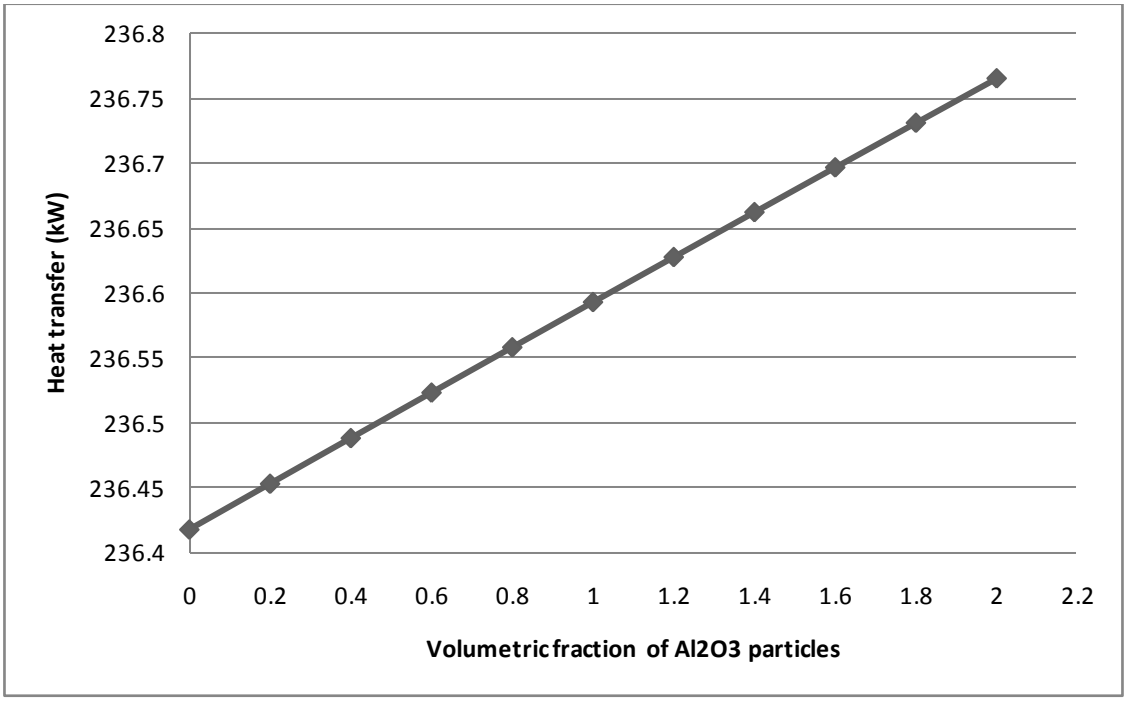

Figure 4.11: Effect of Aluminum Oxide Volume Fraction to Heat Transfer Rate at constant Air and Coolant Reynold Number

CHAPTER 5

Conclusions and Recommendations

This chapter reviews overall conclusions which can be made based on the analysis done in previous chapter. Section 5.1 discusses on the conclusion of the study while suggestion for future works are included in section 5.2

5.1 Conclusion

The conclusions of this study are as below

(a) Ethylene glycol based Aluminum Oxide nanofluid offers higher thermal conductivity, viscosity and density compared to ethylene glycol basefluid.

(b) Ethylene glycol based Aluminum Oxide nanofluid offers lower specific heat compared to ethylene glycol basefluid.

(c) Thermal conductivity, density and viscosity of ethylene glycol based Aluminum Oxide nanofluid increase with volume fraction of Aluminum Oxide particles.

(d) As the volume fraction of Aluminum Oxide nanoparticles (ranging from 0% to 2%) increases, the coolant mass flow rate, heat transfer coefficient and overall heat transfer coefficient based on air side increase at fixed air and coolant Reynold number

(e) As the volume fraction of Aluminum Oxide nanoparticles (ranging from 0% to 2%) increases, the coolant volumetric flow rate, Prandtl number and Nusset number decrease at fixed air and coolant Reynold number

(f) Electric motors which using nanofluid as a coolant offers higher coolant heat transfer coefficient, overall heat transfer coefficient based on air side and heat transfer rate compared to ethylene glycol basefluid coolant

(g) Application of nanofluids in electric motors cooling can reduce heat transfer area for air and it can leads to small size of electric motors in future.

(h) By replacing conventional ethylene glycol with nanofluid as coolant, it can reduce coolant mass and volumetric flow rate, for the same coolant heat transfer coefficient. This will reduce energy consumption for the motor cooling system.

(i) Finally, from this study it proved that by adding aluminum oxide as nanofluid particles into ethylene glycol basefluid can increase the heat transfer rate of electric motors which can lead to higher cooling rate.

5.2 Recommendations

For future work on this topic, the author would like to recommends the following recommendations.

(a) Experimental work should be done to validate to analytical result.

(b) Other types of nanofluids should be considered in cooling of electric motors.

(c) Effect of temperature on thermophysical properties of nanofluid coolant must take into consideration in the analysis.

Bibliography

Abu-Nada, E. (2009). Effects of variable viscosity and thermal conductivity of Al2O3-water nanofluid on heat transfer enhancement in natural convection. *International Journal of Heat and Fluid Flow, 30*(4), 679-690.

Charyulu, D. G., Singh, G., & Sharma, J. K. (1999). Performance evaluation of a radiator in a diesel engine--a case study. *Applied Thermal Engineering, 19*(6), 625-639.

Chein, R., & Huang, G. (2005). Analysis of microchannel heat sink performance using nanofluids. *Applied Thermal Engineering, 25*(17-18), 3104-3114.

Chen, J. A., Wang, D. F., & Zheng, L. Z. (2001). Experimental study of operating performance of a tube-and-fin radiator for vehicles. *Proc Instn Mech Engrs, 215 Part D*, 911918.

Chopkar, M., Das, P. K., & Manna, I. (2006). Synthesis and characterization of nanofluid for advanced heat transfer applications. *Scripta Materialia, 55*(6), 549-552.

Chon, C. H., K. D. Kihm, et al. (2005). "Empirical correlation finding the role of temperature and particle size for nanofluid (Al2O3) thermal conductivity enhancement." Applied Physics Letters**87**(15).

Daungthongsuk, W., & Wongwises, S. (2007). A critical review of convective heat transfer of nanofluids. *Renewable and Sustainable Energy Reviews, 11*(5), 797-817.

Ding, Y., Chen, H., He, Y., Lapkin, A., Yeganeh, M., Siller, L., et al. (2007). Forced convective heat transfer of nanofluids. *Advanced Powder Technology, 18*(6), 813-824.

Eastman, J. A., Choi, S., S, L., Yy, W., & Thompson, L. J. (2001). Anomalously increased effective thermal conductivities of ethylene glycol-based nanofluids containing copper nanoparticles. *Applied Physics Letters, 78*(6), 718-720.

Ganesan, V. (2004). *Internal combustion engine* (2nd ed.). Singapore: McGraw-Hill

Ho, C. J., Chen, M. W., & Li, Z. W. (2008). Numerical simulation of natural convection of nanofluid in a square enclosure: Effects due to uncertainties of viscosity and thermal conductivity. *International Journal of Heat and Mass Transfer, 51*(17-18), 4506-4516.

Ho, C. J., Wei, L. C., & Li, Z. W. (2009). An experimental investigation of forced convective cooling performance of a microchannel heat sink with Al2O3/water nanofluid. *Applied Thermal Engineering, In Press, Corrected Proof*.

Hwang, Y., Lee, J.-K., Lee, J.-K., Jeong, Y.-M., Cheong, S.-i., Ahn, Y.-C., et al. (2008). Production and dispersion stability of nanoparticles in nanofluids. *Powder Technology, 186*(2), 145-153.

Hwang, Y., Lee, J. K., Lee, C. H., Jung, Y. M., Cheong, S. I., Lee, C. G., et al. (2007). Stability and thermal conductivity characteristics of nanofluids. *Thermochimica Acta, 455*(1-2), 70-74.

Hwang, Y. J., Ahn, Y. C., Shin, H. S., Lee, C. G., Kim, G. T., Park, H. S., et al. (2006). Investigation on characteristics of thermal conductivity enhancement of nanofluids. *Current Applied Physics, 6*(6), 1068-1071.

Incopera, F. P., Dewitt, D. P., Bergman, T. L., & Lavine, A. S. (2007). *Fundamentals of heat and mass transfer* (6th ed.). New York: John Wiley&Sons.

Jung, J.-Y., Oh, H.-S., & Kwak, H.-Y. (2009). Forced convective heat transfer of nanofluids in microchannels. *International Journal of Heat and Mass Transfer, 52*(1-2), 466-472.

Kabelac, S., &Kuhnke, J. F. (2006).Heat transfer mechanisms in nanofluids.*Int Heat TransfConf Keynote Papers*.Begell House Inc. Retrieved from http://www.begellhouse.com/proceedings/IHTC13,789240953a0e790c,252a8d9249f570a2.html

Kakaç, S., & Pramuanjaroenkij, A. (2009). Review of convective heat transfer enhancement with nanofluids. *International Journal of Heat and Mass Transfer, 52*(13-14), 3187-3196.

Kays, W. M., & London, A. L. (1984). *Compact heat exchanger* (3rd ed.). United States: McGraw-Hill,Inc.

Keblinski, P., A.Eastman, J., & G.Cahill, D. (2005). Nanofluids for thermal transport. Retrieved 31 August 2009, from http://www.scorec.rpi.edu/REPORTS/2005-41.pdf

Kim, D., Kwon, Y., Cho, Y., Li, C., Cheong, S., Hwang, Y., et al. Convective heat transfer characteristics of nanofluids under laminar and turbulent flow conditions. *Current Applied Physics, In Press, Corrected Proof*.

Kulkarni, D. P., Das, D. K., & Vajjha, R. S. (2009). Application of nanofluids in heating buildings and reducing pollution. *Applied Energy, In Press, Corrected Proof*.

Kulkarni, D. P., Vajjha, R. S., Das, D. K., & Oliva, D. (2008). Application of aluminum oxide nanofluids in diesel electric generator as jacket water coolant. *Applied Thermal Engineering, 28*(14-15), 1774-1781.

Lee, J.-H., Hwang, K. S., Jang, S. P., Lee, B. H., Kim, J. H., Choi, S. U. S., et al. (2008). Effective viscosities and thermal conductivities of aqueous nanofluids containing low volume concentrations of Al2O3 nanoparticles. *International Journal of Heat and Mass Transfer, 51*(11-12), 2651-2656.

Liu, M.-S., Lin, M. C.-C., Tsai, C. Y., & Wang, C.-C. (2006). Enhancement of thermal conductivity with Cu for nanofluids using chemical reduction method. *International Journal of Heat and Mass Transfer, 49*(17-18), 3028-3033.

Mintsa, H. A., Roy, G., Nguyen, C. T., & Doucet, D. (2009). New temperature dependent thermal conductivity data for water-based nanofluids. *International Journal of Thermal Sciences, 48*(2), 363-371.

Murshed, S. M. S., Leong, K. C., & Yang, C. (2008). Thermophysical and electrokinetic properties of nanofluids - A critical review. *Applied Thermal Engineering, 28*(17-18), 2109-2125.

Hi-Dong Chai, Electromechanical Motion Devices, Prentice Hall, 1998

Deng, F. (1999). "An improved iron loss estimation for permanent magnet brushless machines." Ieee Transactions on Energy Conversion**14**(4): 1391-1395.

Feng, Y. J., B. M. Yu, et al. (2007). "The effective thermal conductivity of nanofluids based on the nanolayer and the aggregation of nanoparticles." Journal of Physics D-Applied Physics**40**(10): 3164-3171.

Heris, S. Z., M. N. Esfahany, et al. (2006). "Investigation of CuO/water nanofluid laminar convective heat transfer through a circular tube." Journal of Enhanced Heat Transfer**13**(4): 279-289.

Heris, S. Z., S. G. Etemad, et al. (2006). "Experimental investigation of oxide nanofluids laminar flow convective heat transfer." International Communications in Heat and Mass Transfer**33**(4): 529-535.

Karthikeyan, N. R., J. Philip, et al. (2008). "Effect of clustering on the thermal conductivity of nanofluids." Materials Chemistry and Physics**109**(1): 50-55.

Lee, J. and I. Mudawar (2007). "Assessment of the effectiveness of nanofluids for single-phase and two-phase heat transfer in micro-channels." International Journal of Heat and Mass Transfer**50**(3-4): 452-463.

Pak, B. C. and Y. I. Cho (1998). "Hydrodynamic and heat transfer study of dispersed fluids with submicron metallic oxide particles." Experimental Heat Transfer**11**(2): 151-170.

Ren, Y., H. Xie, et al. (2005). "Effective thermal conductivity of nanofluids containing spherical nanoparticles." Journal of Physics D-Applied Physics**38**(21): 3958-3961.

Tan, F. D., J. L. Vollin, et al. (1995). "A Practical Approach for Magnetic Core-Loss Characterization." Ieee Transactions on Power Electronics**10**(2): 124-130.

Vasu, V., K. R. Krishna, et al. (2009). "Heat transfer with nanofluids for electronic cooling." International Journal of Materials & Product Technology**34**(1-2): 158-171.

Wang, H., L. Gao, et al. (1999). "Preparation of nanoscale alpha-Al2O3 powder by the polyacrylamide gel method." Nanostructured Materials**11**(8): 1263-1267.

Xuan, Y. M. and Q. Li (2000). "Heat transfer enhancement of nanofluids." International Journal of Heat and Fluid Flow**21**(1): 58-64.

Yu, C. J., A. G. Richter, et al. (2000). "Molecular layering in a liquid on a solid substrate: an X-ray reflectivity study." Physica B-Condensed Matter**283**(1-3): 27-31.

Yu, W. and S. U. S. Choi (2003). "The role of interfacial layers in the enhanced thermal conductivity of nanofluids: A renovated Maxwell model." Journal of Nanoparticle Research **5**(1-2): 167-171.

Appendix A

This section reviews sample calculations used in this study

Thermophysical Properties of Nanofluid

Consider 2% Aluminum Oxide + Ethylene glycol nanofluid

(a) *Density*

Given:

Aluminum Oxide volume fraction, φ =2%

Density of ethylene glycol basefluid, ρ_f = 1071kg/m^3

Density of Aluminum Oxide particle, ρ_p = 3970kg/m^3

Hence, density of 2% Aluminum Oxide + Ethylene glycol nanofluid

$\rho_{nf} = (1-\varphi)\rho_f + \varphi\rho_p$

$= (1- 0.02)1071+0.02(3970)= 1128.98 kg/m^3$

(b) *Heat capacity*

Given :

Aluminum Oxide volume fraction, φ =2%

Density of ethylene glycol basefluid, ρ_f = 1071kg/m^3

Density of Aluminum Oxide particle, ρ_p = 3970kg/m^3

Density of 2% Aluminum Oxide + Ethylene glycol nanofluid, ρ_{nf} = 1128.98kg/m^3

Hence, heat capacity of 2% Aluminum Oxide + Ethylene glycol nanofluid

$$C_{nf} = \frac{(1-\varphi)\rho_f C_f + \varphi\rho_p C_p}{\rho_{nf}}$$

$$= \frac{(1-0.02)1071 \times 2682 + 0.02 \times 3970 \times 870.0}{1233.14} = 2554.6 \text{J/kgK}$$

(c) *Viscosity*

Given:

Viscosity of basefluid (Ethylene glycol), μ_f = 0.003066 Ns/m

Aluminum Oxide volume fraction, φ =2%

Hence, viscosity of 2% Aluminum Oxide + Ethylene glycol nanofluid, μ_{nf}

$$\mu_{nf} = \mu_f \frac{1}{(1-\varphi)^{2.5}} = 0.003066 \frac{1}{(1-0.02)^{2.5}} = 0.003225 \text{Ns/m}$$

(d) *Thermal Conductivity*

Aluminum Oxide volume fraction = 2%

Thermal conductivity of Aluminum Oxide particles, k_p =37.84W/mK

Thermal conductivity of basefluid (ethylene glycol) k_f = 0.2622W/mK

Shape factor, n = 3

Hence thermal conductivity of 2% Aluminum Oxide + Ethylene glycol nanofluid

$$k=k_f\left[\frac{k_p+(n-1)k_f-(n-1)\varphi(k_f-k_p)}{k_p+(n-1)k_f+\varphi(k_f-k_p)}\right]$$

$$k=0.261\left[\frac{37.84+(3-1)0.2622-(3-1)0.02(0.2622-37.84)}{37.84+(3-1)0.2622+0.02(0.2622-37.84)}\right]=0.277917\text{W/mK}$$

Calculation of Thermal Performance of Electric Motor

(a) *For air side calculation*

Air Reynold number = 4000

Air viscosity = 0.00001898Ns/m^2

Reynold number, $Re_a=\frac{G_a D_{h,a}}{\mu_a}$

$$4000=\frac{G_a\times 0.00351}{0.00001898}$$

Mass velocity, G_a= 21.62962963

Mass flow rate, $W_a = G_a \times A_{fr} \times \sigma_a = 21.62962963 \times 0.5 \times 0.6 \times 0.78 = 5.0613333$

$$Colburn\ factor, j_a = \frac{0.174}{Re_a^{0.383}} = \frac{0.174}{4000^{0.383}} = 0.007260395$$

Heat capacity, $C_{p,a} = 1007.4 J/kgK$

Prandtl number, Pr = 0.706

$$\text{Heat transfer coefficient}, h_a = \frac{j_a G_a C_{p,a}}{Pr_a^{2/3}} = \frac{0.007260395 \times 21.62962963 \times 1007.4}{0.706^{2/3}}$$

$$= 199.5299837 W/m^2K$$

$$\text{Fin efficiency of plate fin}, \eta_f = \frac{\tanh mL}{mL}$$

Fin length, L = 0.005715m

Thermal conductivity of fin = 398.3 W/m^2K

Fin thickness = 0.0001m

$$m = \sqrt{\frac{2h_a}{kt}} = \sqrt{\frac{2 \times 199.5299837}{398.3 \times 0.0001}} = 100.0953559$$

$$\text{Fin efficiency of plate fin}, \eta_f = \frac{\tanh mL}{mL}$$

$$= \frac{\tanh (100.0953559 \times 0.005715)}{(100.0953559 \times 0.005715)} = 0.903529547$$

Hence total surface temperature effectiveness, η_0

$$\eta_0 = 1.0 - (1.0 - \eta_f) \times \frac{A_f}{A}$$

$= 1.0-(1.0-0.903529547)\times 0.845=0.918482467$

(b) *For coolant side calculation*

Consider 2% Aluminum Oxide + Ethylene glycol nanofluid

Coolant Reynold number = 5000

Hydraulic diameter, $D_{h,nf}$ = 0.00373m

Viscosity of 2% Aluminum Oxide + Ethylene glycol nanofluid, μ_{nf}= 0.003224831Ns/m^2

$$Re_{nf}=\frac{G_{nf}D_{h,nf}}{\mu_{nf}}$$

$$5000=\frac{G_{nf}\times 0.00373}{0.003224831}$$

Coolant mass velocity, G_{nf}=4322.829772/m^2s

$$G_{nf}=\frac{W_{nf}}{A_{fr}\,\sigma_{nf}}$$

$$4280.532=\frac{W_{nf}}{0.4\times 0.6\times 0.129}$$

Coolant mass flow rate, W_{nf}= 133.8348097kg/s

$$\text{Coolant volumetric flow rate, } \nu_{nf}=\frac{W_{nf}}{\rho_{nf}}$$

$$\text{Coolant Prandtl number, } Pr_{nf}=\frac{\mu_{nf}C_{p,nf}}{k_{nf}}$$

$$=\frac{0.003224831\times 2554.564}{0.277917}=29.64204$$

Coolant Nusset number , $Nu_{nf}=0.023Re_{nf}^{0.8}Pr_{nf}^{0.3}$

$=0.023\times5000^{0.8}\times29.64204^{0.3}=57.87304$

Heat transfer coefficient of coolant $h_{nf}=\frac{Nu_{nf}k_{nf}}{D_{h,nf}}=\frac{57.87304\times0.277917}{0.00373}$

$=4312.043$

Overall heat transfer coefficient based on air side, U_a

$$\frac{1}{U_a}=\frac{1}{\eta_o h_a}+\frac{1}{\left(\frac{\alpha_{nf}}{\alpha_a}\right)h_{nf}}$$

$$\frac{1}{U_a}=\frac{1}{0.918482467\times199.5299837}+\frac{1}{\left(\frac{138}{886}\right)4312.043}$$

$U_a = 143.978\ W/m^2K$

Air side capacity rate , $C_a=W_a c_{pa}= 5.0613333\times1007.4=\frac{5098.7872W}{K}$

Coolant side capacity rate ,$C_{nf} = W_{nf}C_{p,nf} = 133.8348\times2554.564=341889.6$

$C_{minimum} = 5098.7872W/K$

$$C^* = \frac{C_{minimum}}{C_{maximum}}$$

$$=\frac{5098.7872}{341889.6}=0.01491355$$

$A_{fr,a}$= Radiator volume $\times\ \alpha_a$

$$NTU = \frac{U_a A_{fr,a}}{C_a} = \frac{143.978 \times 0.12 \times 886}{5098.7872} = 3.002231534$$

Effectiveness , $\varepsilon = 1-\exp\left[\left(\frac{1}{C^*}\right)\right](NTU)^{0.22}\{\exp[-C^*(NTU)^{0.78}]-1\}$

$$=1-\exp\left[\left(\frac{1}{0.01491355^*}\right)\right](3.002231534)^{0.22}\{\exp[-0.01491355^*(3.002231534)^{0.78}]-1\}$$

$= 0.947664102$

Total heat transfer rate , $Q = \varepsilon C_{min}(T_{nf,in} - T_{a,in})$

$= 0.947664102 \times 5098.7872 \times (86.5-37.5) = 236.7649$ kW

Appendix C

In this study, the thermal performance of electric motor using ethylene glycol based Aluminum Oxide nanofluid is investigated analytically. This section reviews the finding calculated from the mathematical formulations.

Thermophysical Properties of Coolant

In this study, ethylene glycol liquid acts as base fluid. Addition of Aluminum Oxide particles will affect its thermal physical properties as shown in Table C1. Properties of nanofluid are calculated from empirical formulation. In this study, the thermal conductivity values from literatures were used in calculating thermal performance of radiator. In Table C.2, the influence of volume fraction of aluminum oxide particles to thermal performance of electric motor were calculated.

Table C.1: Thermal Physical Properties of Ethylene Glycol Based Fluid and Nanofluid

Aluminum oxide volume fraction (%)	Density	Heat capacity	Viscosity	Thermal conductivity
0	1071	2682	0.003066	0.2622
0.2	1076.8	2668.6	0.003081	0.263744
0.4	1082.6	2655.4	0.003097	0.265294
0.6	1088.4	2642.3	0.003112	0.26685
0.8	1094.2	2629.4	0.003128	0.268412
1	1099.9	2616.6	0.003144	0.269981
1.2	1105.8	2603.9	0.00316	0.271556
1.4	1111.6	2591.4	0.003176	0.273137
1.6	1117.4	2579	0.003193	0.274724
1.8	1123.2	2566.7	0.003208	0.276317
2	1128.98	2554.6	0.003225	0.277917

Table C.2: Influence of Volume Fraction of Copper Particles to Thermal Performance of electric motor

Aluminum Oxide volume fraction	Coolant mass velocity	Coolant mass flow rate	Coolant volumetric flow rate	Coolant Prantl number	Coolant Nusselt number	Heat transfer coefficient of coolant	Overall heat transfer coefficient	Heat transfer rate,Q
0	4109.92	127.2431	0.118808	31.3616	58.86041	4137.587	142.6883	236.4184
0.2	4130.541	127.8816	0.118761	31.17835	58.75702	4154.641	142.8181	236.4535
0.4	4151.308	128.5245	0.118719	30.99772	58.65469	4171.78	142.9477	236.4886
0.6	4172.222	129.172	0.118681	30.81967	58.55342	4189.005	143.0771	236.5235
0.8	4193.283	129.824	0.118648	30.64416	58.45318	4206.317	143.2064	236.5584
1	4214.493	130.4807	0.11862	30.47115	58.35398	4223.716	143.3354	236.5931
1.2	4235.854	131.142	0.118596	30.30059	58.2558	4241.204	143.4643	236.6277
1.4	4257.366	131.8081	0.118577	30.13244	58.15862	4258.779	143.593	236.6622
1.6	4279.032	132.4788	0.118562	29.96665	58.06244	4276.444	143.7215	236.6965
1.8	4300.853	133.1544	0.118551	29.8032	57.96725	4294.199	143.8498	236.7308
2	4322.83	133.8348	0.118545	29.64204	57.87304	4312.043	143.978	236.7649